THE UNIVERSITY OF QUEENSLAND

Bachelor of Engineering Thesis

Characterising the Microstructure and Mechanical
Properties of Aerospace β-21S Titanium Alloy During
Thermal Ageing

Student Name: Patrick HAGAN

Course Code: MECH4500

Supervisor: Dr. Michael Bermingham

Submission Date: 28 October 2016

A thesis submitted in partial fulfilment of the requirements of the Bachelor of Engineering
degree in Mechanical Engineering

UQ Engineering

Faculty of Engineering, Architecture and Information Technology

Abstract

A relatively new titanium alloy, nominally β-21S or Timetal 21S (Ti-15 Mo-3 Nb-3 Al- 0.2 Si), is a seen as a viable material for the design of advanced titanium composites due to its improved oxidation, strength and creep resistance. Dr. Michael Bermingham is presently working with a confidential manufacturer to assess the suitability of the alloy, for aerospace engine exhaust applications, at typical operating temperatures between 250-600°C. However, the metallurgical stability or ageing response of this alloy over such a temperature range has not previously been studied in depth.

This body of work therefore aims to characterise changes in the microstructure and mechanical properties of the β-21S alloy during low temperature isothermal ageing at 300 and 450°C, representing typical operating temperatures. Optical microscopy, scanning electron microscopy and microhardness techniques were employed for discrete ageing times up to 9days.

Analysis of microhardness testing data suggested that the ageing behaviour of the alloy was significantly different across the two experimental temperatures. In the case of the 450°C aged samples, a severe rate of hardening was observed after an incubation period of 60mins with a peak hardness of 491Hv ($\sigma_y \approx$ 1473MPa) obtained at 72hours. This represents a 71% increase when compared to the as received, solution treated sample. In comparison, an incubation period of up to 8hrs was noted at 300°C, with a peak hardness of 405Hv ($\sigma_y \approx$ 1215MPa) obtained at 9days. There was no evidence of over-ageing.

The hardness of the alloy is dependent on the decomposition of the β phase into fine intragranular α phase particles which prevent the movement of dislocations or crystallographic defects causing plastic deformation. Ageing of the alloy at 450°C results in fine dispersions of α nucleated within the centre of the grains which rapidly grow towards the grain boundaries over time. There is a fine layer of grain boundary α and adjacent precipitate free zone. The precipitates exhibit a lenticular morphology after 8hrs which coarsens over time as larger particles grow preferentially to smaller ones. At 300°C, growth of the equilibrium α phase is relatively slow due to insufficient thermal activation energy, meaning small atomic mobility and diffusion rate. It is hypothesised that an intermediate phase, ω or β', may have first formed. These nano-sized transitional phase precipitates serve as precursors for the nucleation of α

platelets where there is insufficient thermal energy for direct decomposition of the β phase to equilibrium α.

Rapid increases in the hardness of the alloy, due to the nucleation of fine precipitates, are intrinsically proportional to reductions in the ductility. Embrittlement and cracking may therefore be increasing likely at temperatures around 450°C, as well as at 300°C where the alloy is exposed to longer ageing periods.

Acknowledgements

I would first like to extend an enormous thank you to my project supervisor, Dr. Michael Bermingham, for not only his support but also his constant motivation to produce a thesis of high quality. Michael's extensive knowledge in the field of advanced manufacturing and materials has been invaluable in both interpreting results and negotiating potential problems with the research methodology.

I am also grateful for the help and support provided by Scott Leungen, a winter research student, in the polishing and etching of metal samples. This thanks is extended to Mr. Jonathan Read and the technical staff who support the day-to-day operation of the polishing and microscopy labs.

The task of completing this academic thesis has, at times, been challenging, but with the resources and networks afforded by the University of Queensland, I have been able to further my understanding and overall quality of this report. It is certainly a capstone of my engineering degree.

A final thanks must go to my family and friends for their ongoing support of my academic pursuits.

Contents

List of Figures

List of Tables

Abbreviations

HCP	**H**exagonal **C**lose **P**acked
BCC	**B**ody **C**entred **C**ubic
SEM	**S**canning **E**lectron **M**icroscope
Ti	**Ti**tanium
Mo	**Mo**lybdenum
Nb	**N**io**b**ium
Al	**Al**uminium
Si	**Si**licon
Cr	**Ch**romium
V	**V**anadium
Zr	**Zi**rconium
RPM	**R**evolutions **P**er **M**inute
SN	**S**erial **N**umber
SiC	**Si**licon **C**arbide
HF	**H**ydro**f**luoric
PSI	Pounds Force **P**er **S**quare **I**nch
Hv	**V**ickers **H**ardness
TEM	**T**ransmission **E**lectron **M**icroscope
XRD	**X-R**ay **D**iffraction

List of Symbols

°C	Degrees Celsius
α	Material Phase
β	Material Phase
ω	Transitional material phase
β'	Transitional material phase
ε	Engineering Strain
σ_y	Yield strength

Chapter 1

Introduction

1.1 Research Motivation

β-21S, or Timetal 21S, is a relatively new titanium alloy (Ti-15 Mo-3 Nb-3 Al- 0.2 Si) designed for high temperature applications due to its improved oxidation, strength and creep resistance. Commercial applications in forgings include aerospace ducts, engines, plugs and nozzle assemblies (Wanhill & Barter, 2012). Dr. Michael Bermingham is currently working with a confidential manufacturer to assess the suitability of the solution treated material, for engine exhaust applications, at typical operating temperatures between 250-600°C. Currently, there exists little to no knowledge in the public domain regarding the metallurgical stability or ageing response of this alloy over such a temperature range.

1.1.1 Intended Thesis Contribution

This body of work is intended to fill the hole in existing knowledge, whereby, the microstructure and mechanical properties of the alloy are to be characterised during thermal ageing at 300 and 450°C, which represent typical operating temperatures. An understanding of this behaviour has a number of important implications. Not only can it be used to described the behaviour of the material under operating conditions, including predictions for the likelihood of embrittlement or cracking, but it can also be used as a motivation for further research. That is, the results may be used to establish a focus on better understanding the phase transformations in the β-21S alloy or to suggest where critical operating temperatures may occur. Specific elements of the microstructure and mechanical properties to be investigated, including experimental techniques, are presented with justification in chapter three, Research Methodology.

1.2 Research Aims and Objectives

The aim of this body of work is to investigate the changes in microstructure and mechanical properties during thermal ageing of solution treated β-21S titanium alloy. This is to be achieved

using optical microscopy, scanning electron microscopy and microhardness testing techniques. As previously mentioned, the work is intended to characterise the ageing response of this alloy at typical service temperatures, which has not previously been studied in-depth. To realise the deliverable, the aim is divided into the following objectives. The relative success of the research work in achieving these is discussed in chapter 6, Conclusions.

- To characterise the changes in microstructure following thermal ageing treatment of titanium alloy β-21S. This includes comparing and contrasting the alloy's microstructure across discrete time periods of ageing and between the two experimental temperatures (300 and 450°C).
- To quantify the effects of the microstructural changes, which have strengthening mechanisms, on the mechanical properties of the alloy through microhardness testing.
- To discuss the relationship between the microstructures and mechanical properties.
- To indicate potential modes of in-service failure, including the likelihood of embrittlement and cracking.
- To make recommendations regarding the use of titanium alloy β-21S in service conditions similar to those investigated.

1.3 Project Scope

The research project is scoped to provide an extensive investigation of the microstructure and mechanical properties of β-21S during thermal ageing whilst working within practical limitations imposed by available equipment and time constraints. The following table indicates the research work which falls within the scope of the project and also lists any work outside of such scope.

Table 1.1: Summary of Project Scope

In Scope	Out of Scope
Investigate the changes in microstructure and mechanical properties at discrete time periods of ageing up to 9 days and for two experimental temperatures	As the number of ageing time and temperature permutations is subject to time constraints, investigating additional temperatures and/or increasing the resolution of time data points is outside the project scope.
Employ optical microscopy and SEM techniques to visually characterise the changes in alloy microstructure with ageing time and temperature	Resolve intermediate phase particles which cannot be distinguished by available means of optical and scanning electron microscopy
Investigate the effects of ageing on the alloy's mechanical properties through quantifying the microhardness	Other mechanical testing methods, including determining material strength, ductility and fracture toughness by means of tensile and impact testing
Provide recommendations regarding the metallurgical stability of titanium alloy β-21S in service conditions similar to those investigated	Recommend the suitability of β-21S for any specific industry application(s)

1.4 Summary of Chapters

A statement of the engineering problem, through discussion of the background motivation, has been presented in chapter one within the introduction. This section is intended to give the reader a context or background to the problem, define the aim and objectives of the research and delineate the project scope.

Chapter two presents a review of all relevant literature associated with the project. Fundamental concepts such as precipitation hardening and phase transformations are defined in order to enable the document to be accessible by unfamiliar readers. Existing research into the β-21S alloy is presented.

Chapter three provides an overview of the research methodology with the purpose of justifying all project decisions and assumptions. It also allows all experimental data to be reproducible. The entire methodology from heat treatment to sample preparation, microhardness testing and microscopy is specified.

Chapter four contains the experimental results, including optical microscope and scanning electron microscope images as well as hardness testing results. These findings are discussed in

detail in this chapter, which describes the relationship between the alloy's microstructure and its mechanical properties using the prior art established in chapter two. This allows for the implications of the research, or significance in relation to the commercial applications of β-21S, to be suggested.

Chapter five revisits the aims and objectives of the research project and assesses to what extent they were accomplished. A summary of project limitations, and therefore recommendations for future work, is also discussed.

Chapter 2

Literature Review

2.1 Titanium Alloys

Unalloyed titanium, under ambient conditions, exists as a hexagonal close packed crystal structure or α phase which undergoes an allotropic transformation to a body centred cubic β phase at temperatures above 882°C. Depending on the amount of added alloying elements and volume fraction of β phase, titanium alloys can be classified as either α, α+β or β and near β (Luterjing and Williams, 2007). α+β and β alloys are typical of materials used in aerospace applications due to the potential for higher tensile and fatigue strengths with heat treatment processing.

2.1.1 β Titanium Alloys

β titanium alloys are characterised by retention of the β phase following cooling to room temperature during heat treatment, which is a direct consequence of the total alloying elements (figure 2.1). They may be either stable or metastable; meaning in a state that is not the energy minimum. Compositions of alloying elements which constrain the titanium alloy between the critical lower level to avoid martensite formation (β_C) and the β transus line (β_S) are termed metastable as they will produce fine particles of the α phase upon heat treatment (Polmear, 2007). One mechanism by which to categorize β titanium alloys is to determine the equivalent content of the β stabilising element, molybdenum (>10 wt%). Aluminium has the opposite effect as it is an α phase stabiliser (Kent, Wang, & Dargusch, 2013).

2.1.2 Material Designation

Titanium β-21S or Timetal 21S is a metastable β alloy with designation Ti-15 Mo-3 Nb-3 Al-0.2 Si and is designed for high temperature applications, such as in aircraft engine exhaust plug and nozzle assemblies, due to its improved oxidation and creep resistance. The addition of alloying elements Nb, Al and Si to the Ti-Mo system are specifically targeted at improving oxidation resistance (Agarwal, Bhattachjaree, Ghosal, Nandy, & Sagar, 2008).
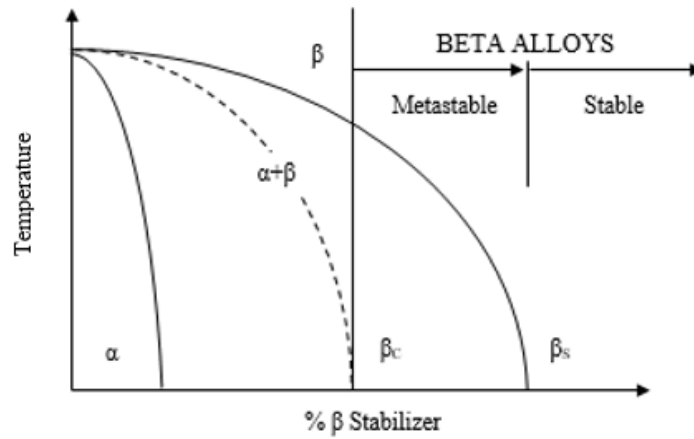
Figure 2.1: Pseudo-binary β isomorphous phase diagram. Adapted from Polmear (2005)

2.2 Solid-solid Phase Transformations

Solid-solid phase transformations are characterised by long range diffusion of a product phase in a parent matrix. The driving force for the nucleation of such a product phase can be expressed in terms of the free energy change in the system, ΔG, and is a function of the nucleus size (Zhang, 2015):

$$\Delta\text{G} = 4\pi r^2 \gamma_{ab} + \frac{4}{3}\pi r^3 (\Delta G_V + \Delta G_S) \qquad \text{(Equation 2.1)}$$

Here ΔG_V is the volume free energy change due to the formation of product phase, ΔG_S is the elastic strain energy per unit volume due to the misfit between the product phase and parent matrix and γ_{ab} is the interfacial energy per unit area due to the introduction of extra interfaces. In the case of solid transformations, the contribution of the elastic strain energy dominates for small sized particles and reduction of the interfacial energy is achieved by assuming a coherent structure (atomic matching of the two phases across the interface). As the particles grow, introduction of misfit dislocations, resulting in a semi-coherent interface, reduce the elastic energy.

The growth rate of the product phase (V) is governed by the temperature and time (t) as demonstrated by the following relationship (Zhang, 2015):

$$V \propto \Delta x \sqrt{\frac{D}{t}}$$ (Equation 2.2)

Here Δx is the supersaturation and D is the diffusion rate. At lower temperatures, there is a greater supersaturation which implies a greater volume free energy change, ΔG_V, and therefore growth rate. However, there is also small atomic mobility and diffusion, lowering such a rate. This balance leads to a maximum growth rate at an intermediate temperature.

2.2.1 Precipitation Hardening (Age Hardening)

Precipitation hardening is a two-stage heat treatment process which produces a microstructure that contains small, dispersed particles or precipitates of a product phase within the original phase matrix as per a solid-solid phase transformation. The first stage is termed solution heat treatment and is characterised by heating an alloy above the solvus temperature (limit of solubility of one solid phase in another) and holding it until formation of a homogeneous solid solution. i.e. solubility of titanium alloy α precipitates in β phase. The metal is subsequently quenched or rapidly cooled to room temperature to form a supersaturated solid solution. The atoms do not have sufficient time to diffuse to prospective nucleation sites, therefore preventing the formation of α precipitates. The second step in the precipitation hardening process is termed ageing and is characterised by heating the supersaturated solid solution below the solvus temperature. Finely dispersed precipitates are produced as atoms diffuse to potential nucleation sites (Smart, 2013).

The decomposition of the supersaturated solid solution often begins with a clustering of solute atoms into a region coherent with the matrix phase. These zones, which are a few atoms thick, are termed Guinier-Preston (GP) zones (Morris, 2001). Although coherent with the parent phase, strain is introduced into the lattice. Certain alloys, including beta-titanium alloys, then form intermediate or transitional precipitates which have definite composition and crystal structure. The formation of the final equilibrium precipitates leads to a loss of coherency within the parent lattice (Smart, 2013).

There are several mechanisms which contribute to an increase in the strength of an alloy following precipitation hardening. These are dependent on the ability of the precipitates to act as obstacles to dislocation motion, that is, preventing the movement of crystallographic defects

which allow slip or plastic deformation to occur. One hardening mechanism is coherency stress hardening which relies on the difference in spacing of the crystal lattice between the matrix and precipitate to generate strain fields around the GP zones (Morris, 2001). This impedes dislocation motion and increases with precipitate size. However, a loss of coherency will result as the coherency strain becomes too large, decreasing the lattice strain. The loss of strain energy contributes to the surface energy of the new boundary.

In the case of precipitate cutting, dislocation motion through a GP zone or precipitate creates new surfaces and increases the volume of solvent/solute bonds. The cutting stresses increase with precipitate size. Dislocation bowing is another hardening mechanism and involves the dislocations bypassing the precipitates by bowing between them and re-joining on the opposite side. This is energetically favourable and leaves behind dislocation 'loops' which repel incoming dislocations (Orowan or dispersion hardening) (Morris, 2001).

As previously stated, the alloy's strength is a function of the ability of its precipitates to act as obstacles to dislocation motion (F) as well as the inter-particle spacing (x_0). Initially during ageing, the strength of the alloy increases as F similarly increases and x_0 decreases. However, at some ageing time, x_0 will increase as large precipitates grow preferentially to smaller ones. When the precipitates can no longer be cut by the dislocations, bypassing of the precipitates occurs and the alloy experiences a reduction in strength.

2.3 Heat Treatment of β Titanium Alloys

2.3.1 Phase Transformations in β Ti Alloys

In metastable β titanium alloys, several phase transformations can take place with each influenced by the alloy composition and ageing temperature. An equilibrium alpha phase forms during isothermal ageing below the β transus temperature as well as during slow cooling from the β field. This α phase can be either categorised as type 1, whereby it obeys the Burgers orientation relation with the β matrix, or type 2 with a $\{10\bar{1}2\}<10\bar{1}1>$ twin orientation with respect to Burgers α (Chaudhuri & Perepezko, 1994). The direct decomposition of the β phase to equilibrium α is observed only at sufficiently large temperatures due to the difficulty of nucleating HCP α phase from the BCC β matrix. As a result, intermediate decomposition products or transitional phases are often formed (Polmear, 2005).

Two transitional phases have also been observed in metastable β titanium alloys. An ω phase may form during quenching (athermal ω) or during low temperature ageing (isothermal ω) (Chaudhuri & Perepezko, 1994). The morphology of this phase is heavily dependent on the misfit between the precipitate and BCC structure of the matrix. In low misfit alloys, an ellipsoidal ω phase persists whilst in high misfit alloys a cuboidal phase is formed. It was also found that in alloys with β stabilising elements, a β' transitional phase is formed. This is due to the separation of the BCC phase into two BCC phases of different compositions in these alloys (Leyens and Peters, 2003). If silicon is an alloying element, silicides may also be found. Low temperature ageing can therefore be said to result in the following two phase transformations, depending on ageing time and temperatures (Polmear, 2007):

(1) $\beta \rightarrow \beta + \omega \rightarrow \beta + \omega + \alpha \rightarrow \beta + \alpha$ (Solute lean, metastable β Ti-alloys)

(2) $\beta \rightarrow \beta + \beta' \rightarrow \beta + \beta' + \alpha \rightarrow \beta + \alpha$ (Solute rich, metastable β Ti-alloys)

The mechanism of formation of the equilibrium α phase, either through direct nucleation or indirectly from ω and β' transitional phases, is deterministic of its morphology and distribution with implications for the mechanical properties. Direct nucleation can exhibit as either of two morphologies. Coarse Widmanstatten plates of α occur in dilute binary alloys aged above the limit of ω formation and in alloying systems containing aluminium (Polmear, 2007). In alloys containing large amounts of β-stabilising elements, and which are aged at temperatures above which phase separation of β takes place, a fine dispersion of α precipitates is observed (Luterjing and Williams, 2007). Heterogeneous nucleation, that is nucleation of a continuous layer occurring on grain boundaries, is common.

The nucleation mechanism of equilibrium α from the β matrix containing ω transitional phase particles is dependent upon both the relative misfit and ageing temperature. Low misfit results in heterogeneous nucleation at the grain boundaries by cellular reaction whilst high misfit results in nucleation at the β/ω interfaces (Chaudhuri & Perepezko, 1994). In the case of β' transitional phase formation, nucleation of the α phase occurs within the β particles. Consequently, the α phase transformation is dependent upon the β' distribution and is therefore uniformly dispersed and tightly spaced (Polmear, 2007).

2.3.2 Mechanical Properties

In the case of β titanium alloys, the mechanical properties are directly dependent on such factors as the morphology, volume fraction, size and distribution of the α phase in the β matrix, following formation during isothermal ageing below the β transus temperature. This is in keeping with classical precipitation hardening or age hardening theory (section 2.2.1); fine, hard particles within the microstructure result in greater resistance to dislocation slip and therefore have a higher hardening effect.

The yield stress of the alloy is proportional to the inverse of the inter-particle distance (x_0), as defined by Orowan's relationship, for incoherent α precipitates. For a given ageing temperature, the maximum yield strength is achieved once precipitation of the equilibrium volume fraction of α has occurred. At greater ageing temperatures, the maximum attainable yield strength decreases as a result of a reduced equilibrium volume fraction. However, the time to reach such a maximum is shortened. The alloy hardness, or resistance of the metal to plastic deformation, is fundamentally related to the precipitation hardening response and therefore the yield strength. The Vickers hardness provides a good estimate of the yield strength by the following relationship (Kent, Wang, Wang, & Dargusch, 2012):

$$\sigma_y \cong \frac{H_v}{3} \qquad\qquad\qquad\qquad\qquad \text{(Equation 2.3)}$$

Nucleation of the α phase commonly occurs preferentially at the grain boundaries, due to the high interfacial energy and relatively weak bonding, where it forms a continuous layer. There is a precipitate free zone adjacent to this layer which is free of α platelets and is therefore soft in comparison to the precipitation hardened matrix (Luterjing and Williams, 2007). The mechanical properties of the alloy have been shown to be dependent both upon the strength of the age hardened matrix as well as the slip length in the soft zone (β grain size).

The plasticity of the alloy has been shown in several studies, such as that by Luterjing and Williams (2007), to be largely controlled by the preferential plastic deformation along the grain boundary α film. Where there is a soft precipitate free layer adjacent to the grain boundary, localised increases in the dislocation slip length allow substantial pile up of dislocations and subsequent crack nucleation. This preferred plastic deformation may be severely concentrated

if there is a significant strength difference between the age hardened matrix and soft zones. The presence of coarser and more widely dispersed precipitates at the grain boundaries, when compared with the β matrix strengthened by fine equilibrium α, also results in localised increases in available slip length. This is a maximum once the long axis of such α plates is parallel with the maximum resolved shear stress, resulting in crack formation and a loss in plasticity (Shi, Guo, Liu, Wang, & Yao, 2015). Yao et al. (2015) and Luterjing and Williams (2007) also observed fast micro-crack propagation where fine coherent and semi-coherent precipitates had been cut by dislocations, leading to the formation of severe, planar slip bands.

2.4 Effect of Heat Treatment on the Microstructure and Mechanical Properties of β-21S

2.4.1 Scope of Existing Research

Within the existing body of research, the microstructural development of β titanium alloys is not as extensively described as phase transformations in β+α alloys. Whilst studies of Timetal 21S have aimed to describe such changes in microstructure under various heat treatment techniques, the metallurgical stability of this material at operating temperatures between 200-600°C has not been fully considered. As these are typical service temperatures of the material, it is important to characterise the change in microstructure and physical properties with time over such a range.

2.4.2 Microstructure Development

Chaudhuri and Perepezko (1994) identified the formation of α, ω and silicide precipitate phases in Timetal 21S under several heat treatment methods. Solution treatment at 900°C for 6-48hours of a bulk alloy worked below β transus, followed by air cooling, resulted in recrystallised and non-recrystallised regions of the microstructure. The non-recrystallised regions were characterised by high α precipitate density which could be attributed to more sites for potential nucleation provided by the substructure. It was also shown that recrystallization results from the large deformation of small grains in the initial, non-uniform structure. Heat treatment then promotes recrystallization and growth in these smaller grains whilst the larger ones simply undergo recovery (Chaudhuri & Perepezko, 1994).

Chaudhuri and Perepezko (1994) also demonstrated the formation of an athermal ω phase and silicide precipitates following quenching from the solution treatment temperature of 900°C. Subsequent high temperature ageing at 600°C resulted in precipitation of the α phase, which occurred more slowly in the recrystallised regions. In contrast, low temperature ageing at 350°C yielded an additional isothermal ω phase characterised by an ellipsoidal morphology.

Huang, Cuddy, Goel, and Richards (1994) also investigated the effects of ageing on the microstructural development of titanium alloy β-21S. It was observed that precipitation of the α phase occurs on the grain boundaries during high temperature aging at 650°C and within the grains during low temperature aging at 400°C. In the latter case, progression toward the grain boundaries was noted at aging times above 8 hours. Uniform precipitation occurred at an isothermal aging temperature of 538°C for 8 hours. This was consistent with results detailed by Agarwal et al. (2004) who conducted ageing (8 hours) of Timetal 21S at 540 and 590°C following solution treatment at 845°C for 30 minutes. A dense aggregate of α precipitates was noted with continuous grain boundary α at the higher temperature.

Chapter 3

Research Methodology

3.1 Overview

A Ti-15 Mo-3 Nb-3 Al- 0.2 Si (% by mass) β-titanium alloy was received as a wrought sheet from which small samples (approximately 5x10x1mm) were cut. Isothermal ageing of the samples at both a specified furnace temperature of 300°C and 450°C was conducted for varying time periods (0, 0.25, 0.5, 1, 1.5, 4, 8, 24, 72 and 216 hours). Three samples were obtained for each temperature and time permutation. This was followed by air cooling to room temperature. Each group of samples was mounted in Bakelite resin. The Vickers microhardness of the samples was tested after a standard metallographic process of mechanical grinding and polishing. Five data points on each sample, amounting to fifteen for the specified temperature and ageing time, were obtained. The microstructural development of the alloy was examined by means of optical microscopy and scanning electron microscopy (SEM) following etching in Kroll's reagent.

3.2 Sample Preparation

Small samples (approximately 5x10x1mm) of an as supplied, solution treated, wrought sheet of β-21S titanium alloy were initially cut using a guillotine. To standardise the experimental testing, and ensure consistent properties due to the material's anisotropy, the edge perpendicular to the long transverse side of the sheet was utilised for this research. This orientation is shown in the following schematic diagram. Work hardening at this surface due to the shear stress imposed by the guillotine was seen as a potential source of error and so the samples were required to be well ground following isothermal ageing.
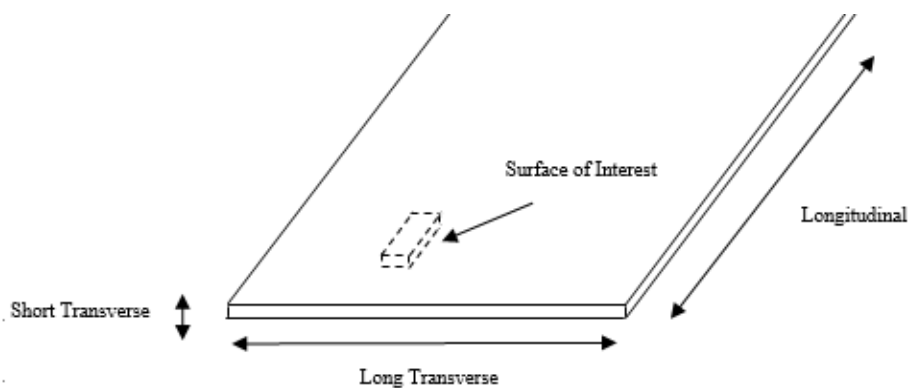
Figure 3.1: Schematic diagram showing a representative sample and experimental surface

Isothermal ageing of the samples was conducted at both a specified furnace temperature of 300°C and 450°C for varying time periods (0, 0.25, 0.5, 1, 1.5, 4, 8, 24, 72 and 216 hours). The following apparatus was utilised:

- Furnace: MV (MIHM-VOGT) GmbH and Co.
  Type: GLP6-U
  S/N: 45299

Three samples were obtained for each temperature and time permutation. This was followed by air cooling to room temperature. The ageing temperatures were chosen to reflect typical service conditions for the titanium alloy, forming part of a wider study by Dr. Michael Bermingham aiming to produce similar data for temperature intervals of 50°C in the range of 300 to 550°C. The ageing times reproduced previous literature with the aim of characterising the initial precipitation of α phase particles and achieving a peak hardness. For instance, a similar study by Kent et al. (2012) identified over-ageing of a new metastable β titanium alloy after only five hours for isothermal ageing temperatures above 400°C.

Preparation of the samples for microhardness testing was then achieved by mounting the samples in LECO black bakelite powder under a mould temperature between 130-180°C and mould pressure of 3800-4400psi. A cure time of 7-10mins was required. This was followed by a standard metallographic procedure of mechanical grinding and polishing as illustrated in table 3.1. The apparatus used in this process is as follows:

- Struers Hot Mounting Press
  Type: Citopress- 30
  S/N: 4172 10470 000

- Struers Specimen Mover (Grinding and Polishing)
  Type: TegraForce-5 and Tegradoser-5
  S/N: 4174 06187 000

Table 3.1: Preparation Procedure for Titanium Samples

Iteration	Surface/ Abrasive	Disc Rotation Speed (rpm)	Sample holder speed (rpm)/ Direction	Load (N)	Time (min.)
1	Wet grind with 120 grit SiC paper	240	240/Comp.	20	2
2	Wet grind with 320 grit SiC paper	200	200/Comp.	15	1
3	Wet grind with 600 grit SiC paper	150	Comp.	15	1
4	Wet grind with 1200 grit SiC paper	150	Comp.	15	1.5
5	Wet grind with 4000 grit SiC paper	240	Manual	Manual	Manual
6	MD-Chem with manual OP-S suspension (20% hydrogen peroxide)	150	150/Comp.	15	10m
7	MD-Chem with manual water application	150	150/Comp.	15	0.75

Notes
- Load is per specimen (multiply by 6 for force on sample holder)
- Complementary rotation (comp.) means sample holder rotates in the same direction as the plate
- Contra-rotation (contra.) means sample holder rotates in the opposite direction to that of the plate
- Samples were cleaned with ethanol, and all equipment washed, between iterations

3.3 Microhardness Testing

The microhardness or resistance of the β-21S alloy to plastic deformation by indentation, quantified as the Vickers hardness, was determined using the following testing apparatus:

- Struers Microhardness Testing
  Type: Duramin
  S/N: 4174 10579 000

The apparatus was utilised by applying a 100gm load over a 12s time interval, with a square-based diamond pyramid indenter. The diagonals of the subsequent indentation were measured using optical microscopy to determine the Vickers hardness. This process was conducted for five data points on each sample, amounting to fifteen for the specified temperature and ageing time. The data points were taken across the full length of the samples, and at different distances from the mould/metal interface, to ensure results were representative of the entire surface. Prior to commencing the testing, the apparatus was calibrated using a 241HV test block [100 gm load]. This procedure was conducted twice, both for the 300°C aged samples and 450°C aged samples, with all data shown below in the following table.

Table 3.2: Calibration Summary for Microhardness Testing

Test No.	Calibration 1: 300°C (HV)	Calibration 2: 450°C (HV)
1	240	232
2	243	242
3	245	227
4	236	231
5	236	232
6	254	240
Average, $\bar{x}$	**242.33**	**234**
Standard Deviation, σ	**6.77**	**5.76**

Microhardness testing was seen as a viable technique by which to efficiently ascertain the ageing behaviour of the alloy across several temperature and time combinations. As suggested in the chapter 2 literature review, the alloy hardness is fundamentally related to the precipitation hardening response and can therefore be used to estimate the strength. This precluded the use of other mechanical testing techniques, such as tensile and impact testing.

3.4 Optical Microscopy and Scanning Electron Microscopy

In order to distinguish microstructural features, etching was conducted using a derivation of Kroll's reagent consisting of 5% HF, 30% HNO_3 and remaining balance H_2O. This was intended to reveal such properties as how and where (nucleation sites) precipitation occurs, morphology, volume fraction, size and distribution of α precipitates in the β matrix. Characterisation of the microstructural features was achieved by means of optical microscope and scanning electron microscope techniques using the following equipment. However, as noted in the project scope, the intermediate ω and β' phase particles can only be observed on a nano-scale and are therefore not expected to be resolved or distinguished between using optical and SEM techniques.

- Reichert-Jung Optical Microscope
  Type: Polyvar MET
  Image Capture: Canon EOS 5D MARK 2 Camera
  Ocular: 1
  S/N: 1350 04899

- Hitachi Tabletop Microscope
  Type: TM3030 Scanning Electron Microscope
  S/N: 55619

Chapter 4

Discussion of Experimental Results

4.1 Microstructure Analysis

4.1.1 Optical Microscopy: Microstructural Development During Isothermal Ageing at 450°C

The following figures 4.1 through 4.7 show the optical microscope images for the 450°C isothermally aged samples for ageing times ranging from as-received to 9 days. As can be seen in figure 4.1, the grains are typically 20-50µm in diameter and are equiaxed as evidenced by their polygonal shape. This is expected in highly β stabilised alloys which have been solution treated above the beta transus temperature and quenched to obtain a fully β structure. There is an incubation period of 60-90 minutes before equilibrium α precipitates are initiated within the β grains. Within this incubation time, a limited fraction of the α phase precipitated on the initial β grain boundaries. This can be attributed to the high interfacial energy and relatively weak bonding at the grain boundaries, making them preferred sites for heterogeneous nucleation.

Figure 4.2 shows the microstructure of the 90 minute aged samples which displays equilibrium α particles having nucleated on the pre-existing grain boundary as well as uniformly within the matrix. The equilibrium α displays a variety of different morphologies and sizes depending on the ageing time. Initially, precipitates exhibit a Widmanstatten star-shaped morphology or clustering of fine α plates. These form throughout the grains and along the grain boundaries. Earlier research has suggested that such low temperature ageing is likely to produce a large number of nano-sized transitional phase precipitates in the matrix (Luterjing and Williams, 2007). These metastable particles serve as precursors for the nucleation of α platelets when there is insufficient thermal energy to decompose the β phase directly to equilibrium α. It is possible that the fine α precipitates observed towards the centre of the grains may have formed by an extension of one of these two transitional mechanisms (ω or β') or that the transitional particles acted as nucleation sites for the precipitation of α particles.
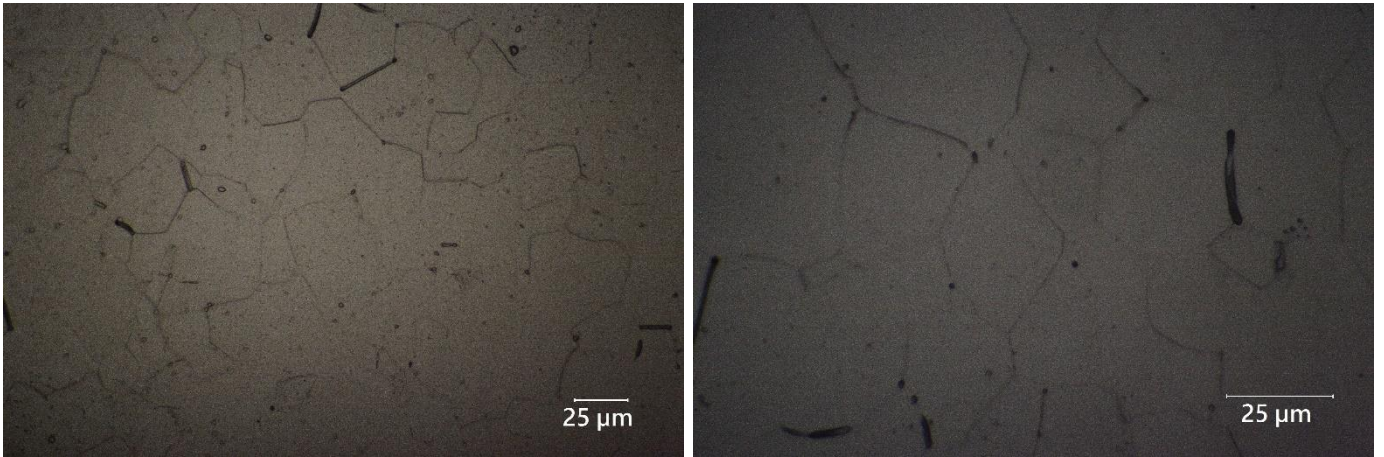
Figure 4.1: Optical microscope images of (a) As received, solution heat treated sample at 50x magnification and (b) 450°C, 30m aged sample at 100x magnification
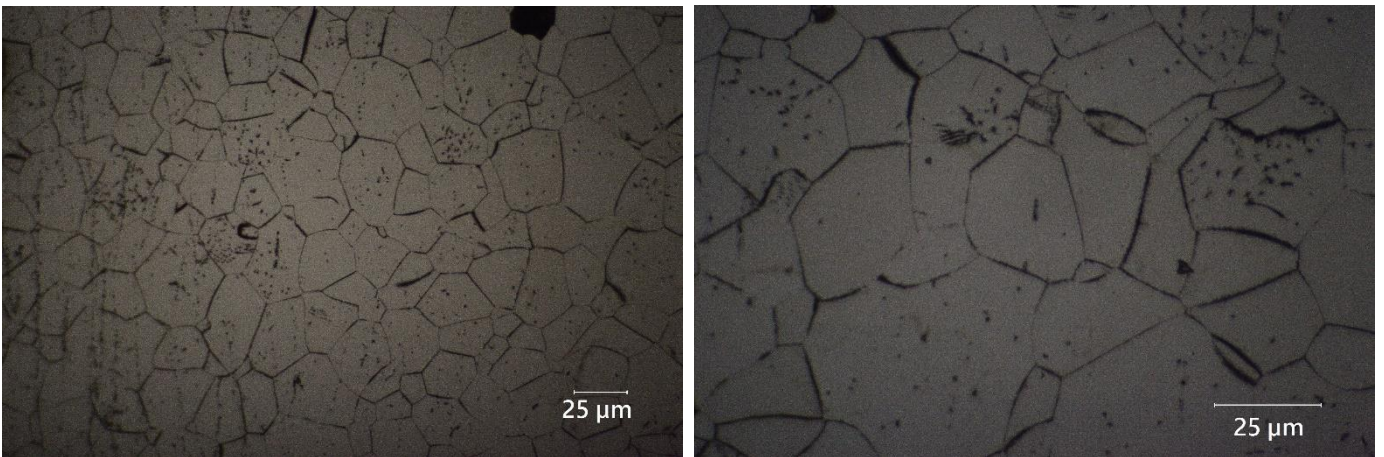

Figure 4.2: Optical microscope images of 450°C, 90m aged sample at (a) 50x and (b) 100x magnification
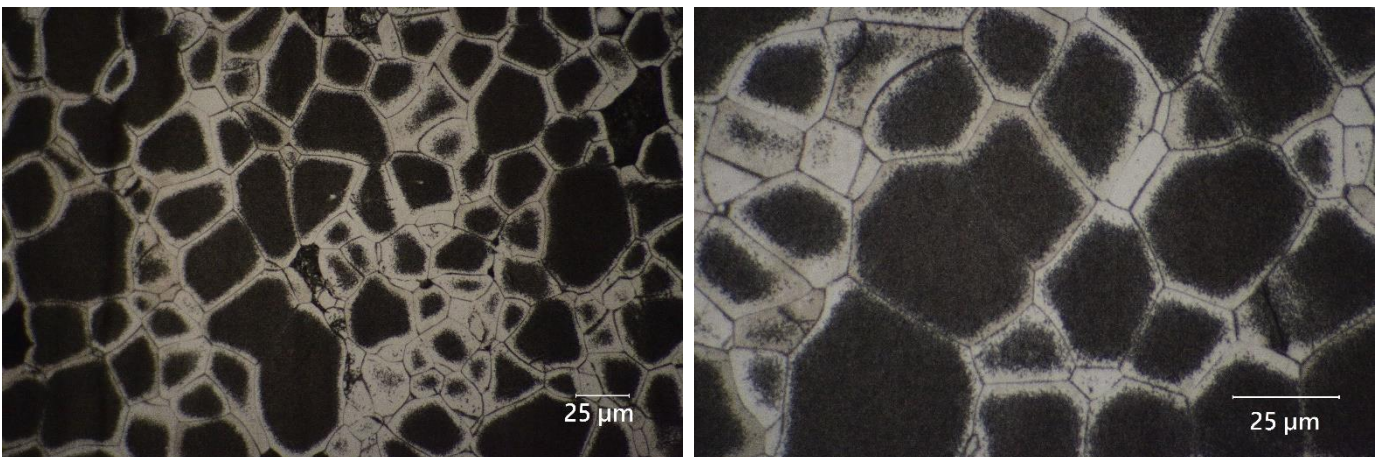

Figure 4.3: Optical microscope images of 450°C, 4h aged sample at (a) 50x and (b) 100x magnification

Figure 4.4: Optical microscope images of 450°C, 8h aged sample at (a) 50x and (b) 100x magnification

Figure 4.5: Optical microscope images of 450°C, 24h aged sample at (a) 50x and (b) 100x magnification
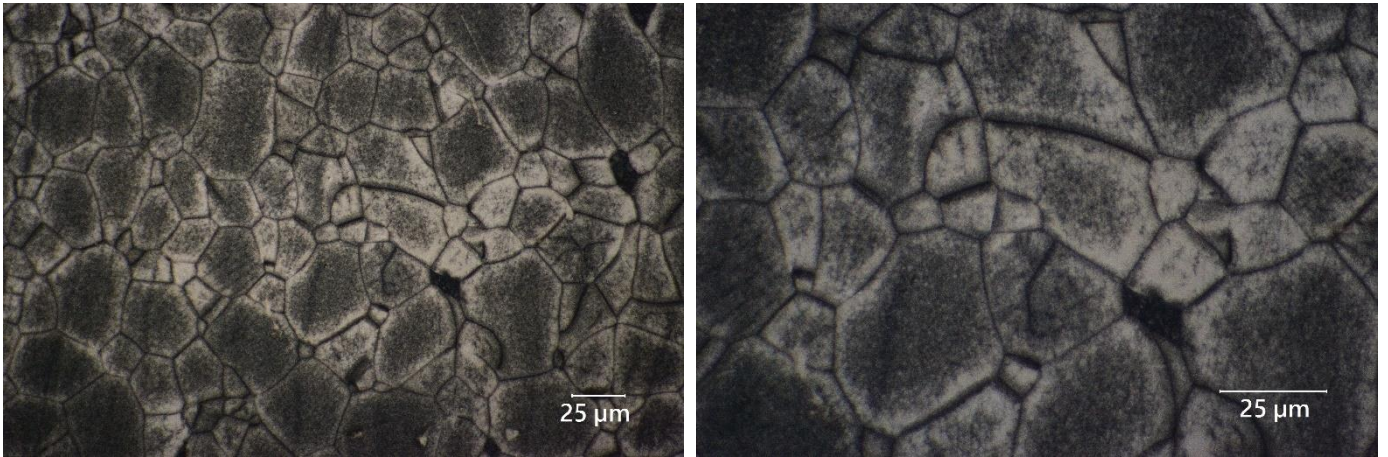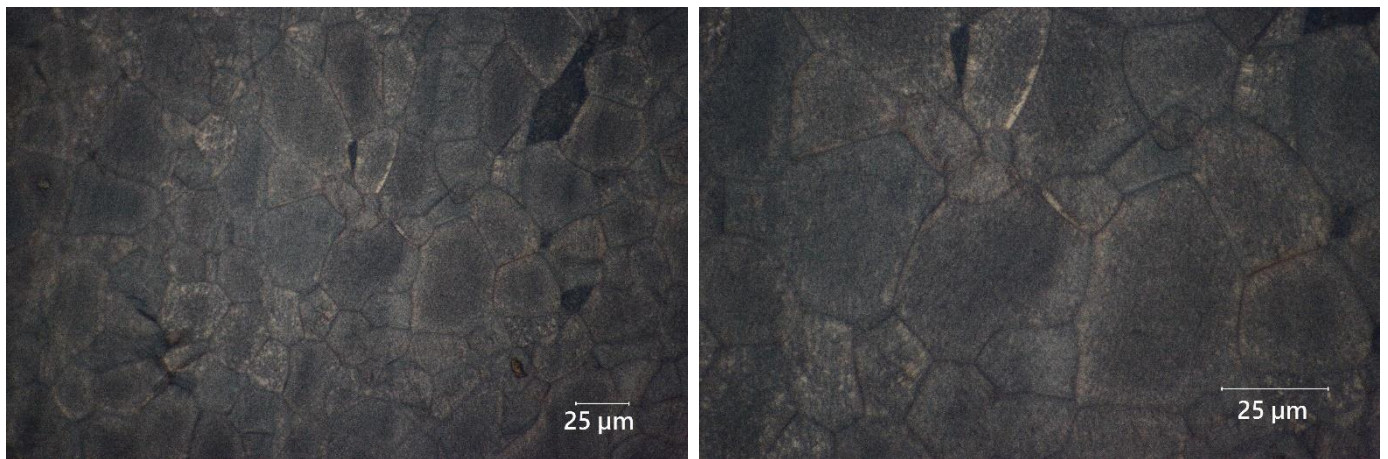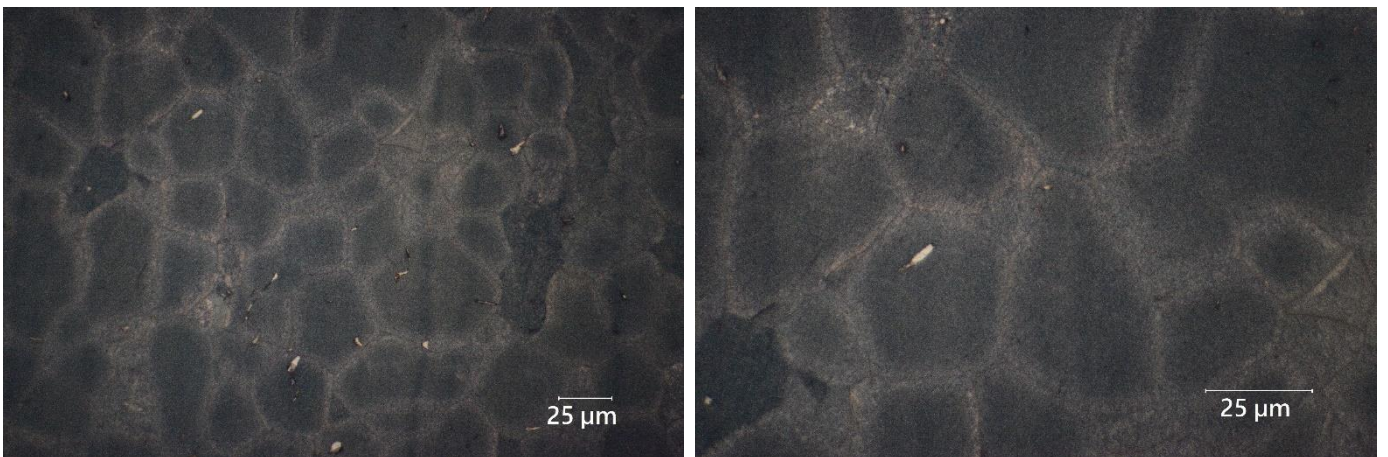

Figure 4.6: Optical microscope images of 450°C, 72h aged sample at (a) 50x and (b) 100x magnification

Characterising the Microstructure and Properties of β-21S Titanium Alloy During Ageing | 20
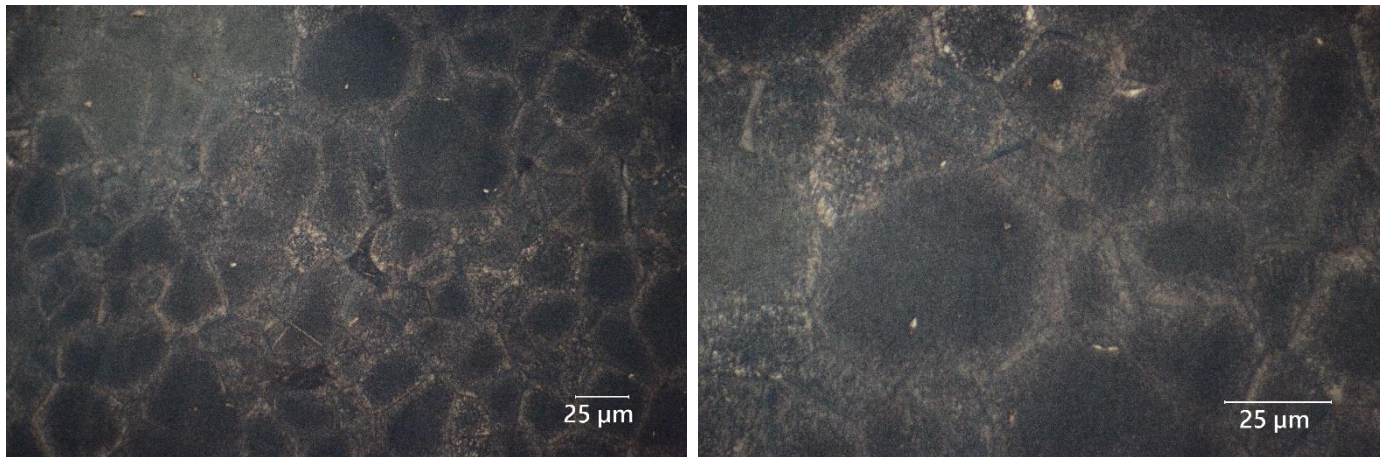
Figure 4.7: Optical microscope images of 450°C, 9d aged sample at (a) 50x and (b) 100x magnification

During the initial ageing process, there is also evidence for preferential precipitation within some grains due to the rejection of α forming elements to these grains. This chemical segregation is likely to have occurred during manufacturing of the as supplied, solution treated sheet. Another noticeable behaviour is heterogeneous nucleation along dislocation lines. This is most evident towards the edge of the sample which is most vulnerable to work hardening or cold working due to the shear stresses imposed by cutting using the guillotine. Again, this heterogeneous nucleation is due to the precipitation of α particles with faster kinetics than for the dispersions of intragranular α.

After an ageing time of 4h (as seen in figure 4.3), the precipitation of the equilibrium α phase, which had occurred homogeneously within the centre of the grains, progressed towards the grain boundaries. As the α phase particles appear finer, there is evidence for decomposition of the large Widmanstatten star morphology and/or nucleation as an extension of the transitional phase. Adjacent to the continuous α layer at the grain boundaries is a so called precipitate free zone which is removed of any α platelets and is therefore soft with respect to the age hardened matrix. The formation of this precipitate free zone can be attributed to the rejection of β phase stabilising elements, namely Mo, V and Cr, during heterogeneous nucleation and growth of the thin grain boundary film. This may have implications for the ductility and fracture mechanics of the alloy as localised increases in dislocation slip length allow substantial pile-up of dislocations and subsequent crack nucleation (Kent et al., 2012).

At greater ageing times, the precipitates present as fine alpha platelets which have a lenticular or acicular morphology. They are observed to grow in size and coarsen. Another important observation is the growth of α precipitates from the centre of the grains towards the grain boundary, reducing the size of the precipitate free zone. A maximum volume fraction of equilibrium alpha within the β grains is obtained between ageing times of 24 and 72h (figures 4.5 and 4.6). After 9 days (figure 4.7), there is significant coarsening of the α precipitates as larger particles consume smaller ones to decrease the total interface area.

4.1.2 Optical Microscopy: Microstructural Development During Isothermal Ageing at 300°C

The microstructural development of the β-21S alloy during isothermal ageing at 300°C is illustrated in the following figures 4.8 through 4.12. Ageing times ranging from the as-received sample to 9days are shown. As can be seen in figure 4.8, the microstructure exhibits equiaxed grains, with polygonal shape, which are typically 20-50µm in diameter. These grain appear as fully β structures over an incubation period of 24-72 hours before equilibrium α precipitates are initiated. When compared to the higher ageing temperature of 450°C, there is lower thermal activation energy, meaning small atomic mobility and diffusion rate. There is slower long-range diffusion of atoms, necessary to achieve equilibrium α phase growth and composition, to potential nucleation sites.

Figure 4.8: Optical microscope images of 300°C aged samples at 50x magnification for (a) As-received and (b) 30mins

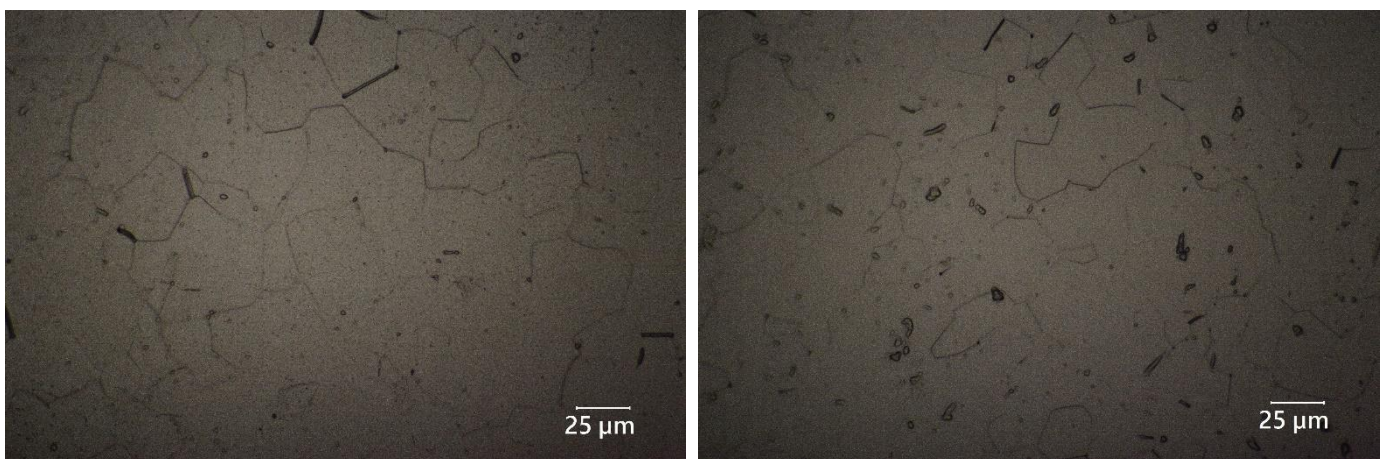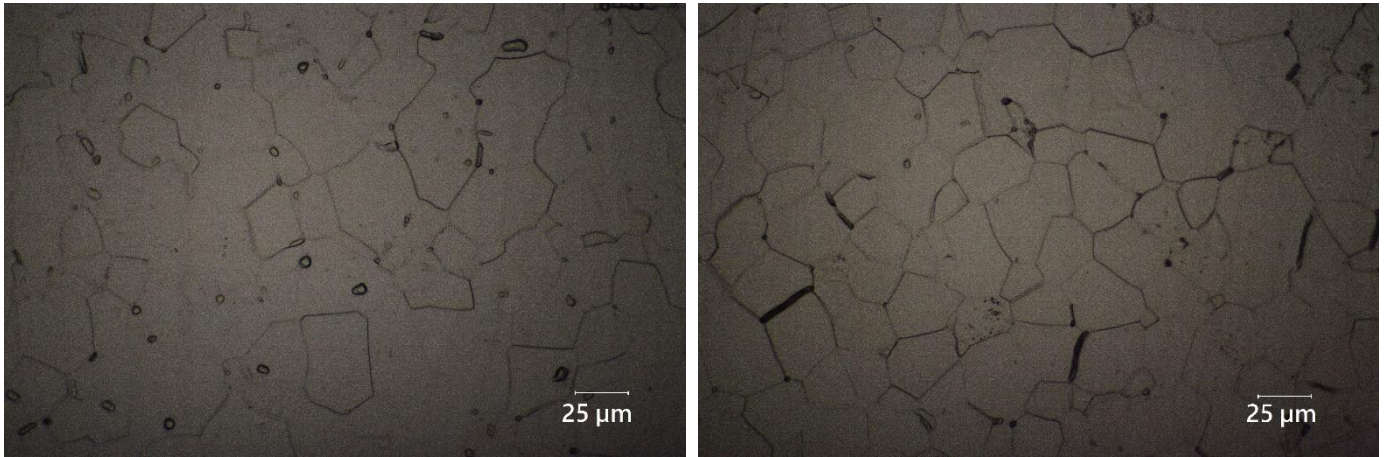*Figure 4.9: Optical microscope images of 300°C aged samples at 50x magnification for (a) 60mins and (b) 4hrs*
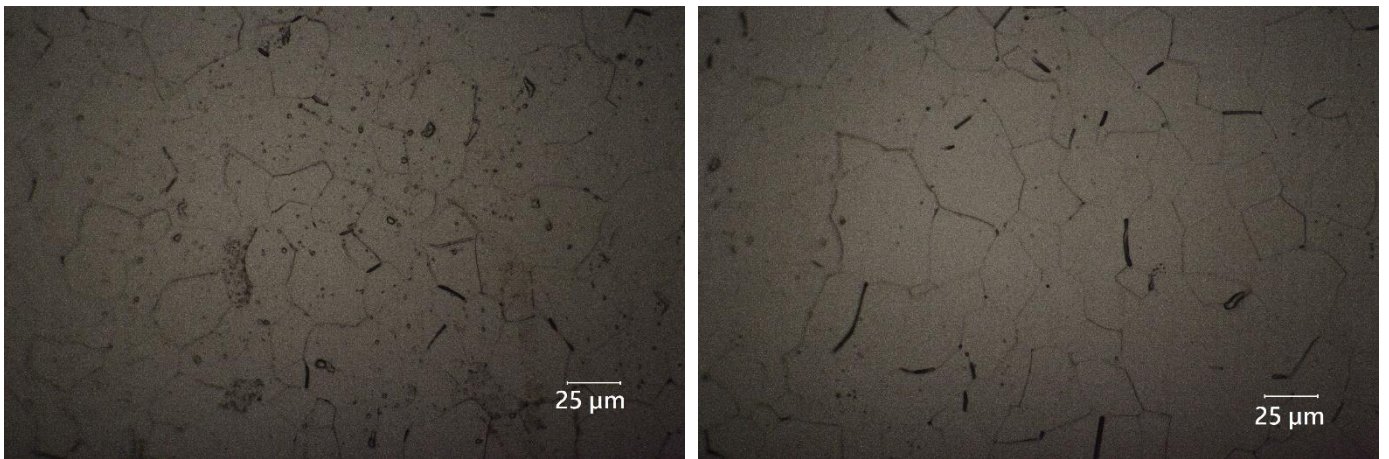

Figure 4.10: Optical microscope images of 300°C aged samples at 50x magnification for (a) 8hrs and (b) 24hrs
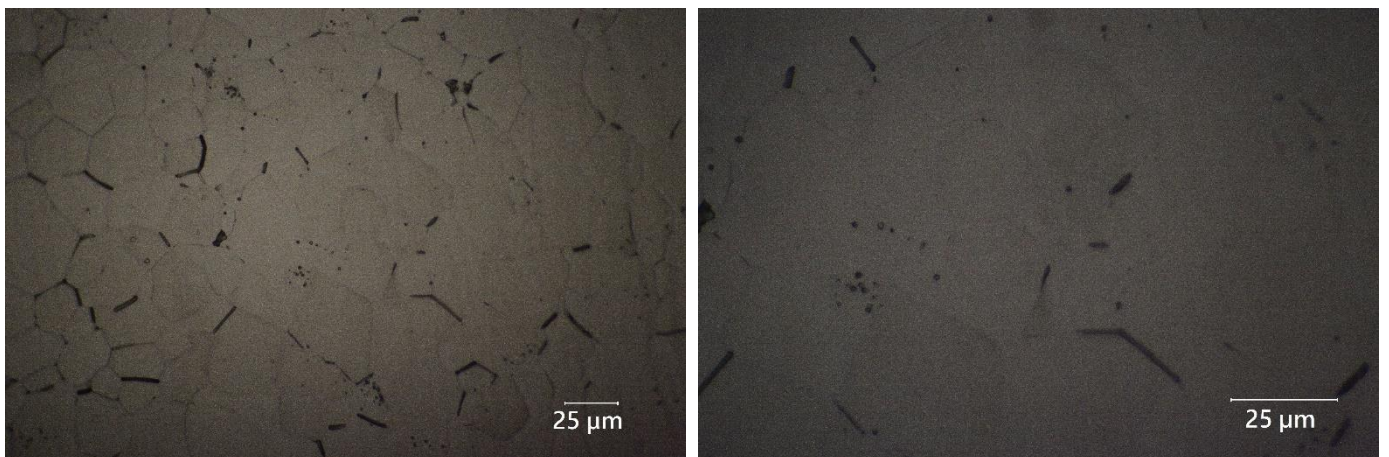

Figure 4.11: Optical microscope images of 300°C, 72h aged sample at (a) 50x and (b) 100x magnification
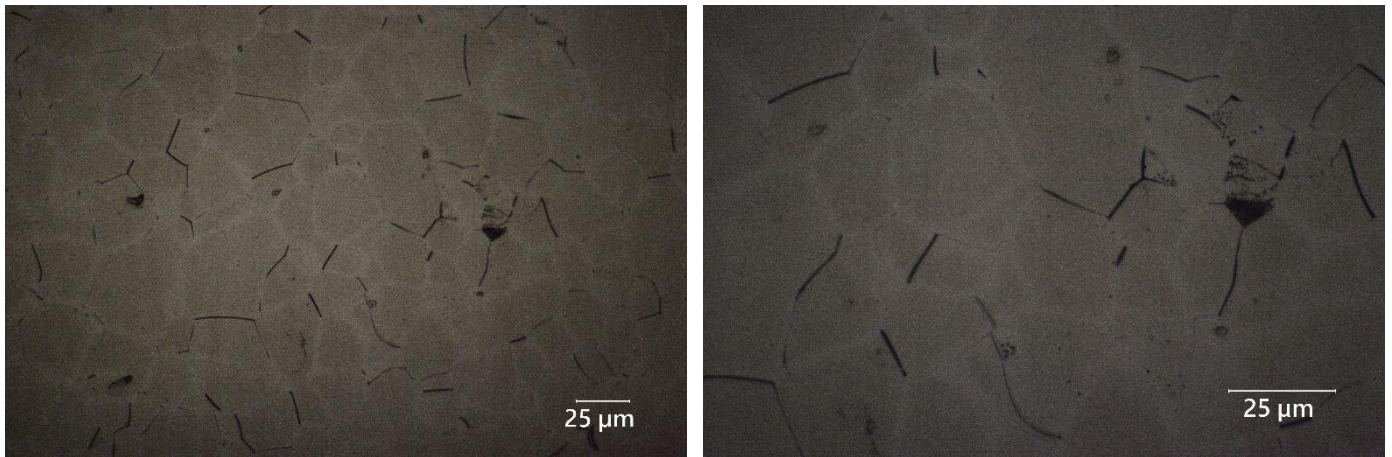
Figure 4.12: Optical microscope images of 300°C, 9 days aged sample at (a) 50x and (b) 100x magnification

From 24 hours, the microstructure exhibits a uniform, fine dispersion of particles within the β matrix. These are significantly smaller than 1μm based on the resolution of the optical microscopy. An explanation for the appearance of a finer, more even distribution of precipitates is the formation of the metastable ω or β' transitional phases. Research has suggested that low temperature ageing in the range 100-500°C is likely to produce a large number of these nano-sized transitional phase precipitates in the matrix (Luterjing and Williams, 2007). These metastable particles serve as precursors for the nucleation of α platelets. As these are beyond the resolution of the optical microscope, the fine particles are suggested to be equilibrium α. It is possible that these α precipitates may have formed by an extension of one of these two transitional mechanisms (ω or β') or that the transitional particles acted as nucleation sites for the precipitation of α particles. At higher temperatures, such as in the case of the 450°C aged samples, there is less opportunity for the formation of the ω or β' precipitates to facilitate intragranular nucleation of the equilibrium α phase. This subsequently results in an increased likelihood for nucleation of α particles as side plates at α/β interfaces.

At longer ageing times of 72h and 9 days, as seen in figures 4.11 and 4.12, larger α precipitates have begun to grow preferentially within certain grains. Again, this is due to chemical segregation and the rejection of α forming elements to these grains. This is also evidence that further ageing is likely to result in precipitate growth with implications for increased strength and hardness consistent with precipitation hardening theory. However, further ageing would need to be conducted to determine when the equilibrium volume fraction of α and peak hardness is obtained.

Another important observation is the formation of precipitate free zones adjacent to the β grain boundaries. These are attributed to the rejection of β phase stabilising elements, namely Mo, V and Cr, during heterogeneous nucleation and growth of the thin grain boundary film. Again, this could be expected to affect the fracture behaviour and ductility of the alloy due to increases in slip length within these regions (Kent et al., 2012).

4.1.3 Scanning Electron Microscopy

Scanning electron microscope imaging was conducted on several samples (figures 4.13-4.15), consolidating the results of the microstructural development detailed using optical microscopy as well as providing further details regarding the size and morphology of the equilibrium α phase precipitates. The results of the 450°C isothermal ageing showed a classical precipitation hardening response; nucleation and growth of fine equilibrium alpha precipitates which increase in volume fraction and coarsen at extended ageing times. As previously mentioned, precipitation of the α phase is observed to occur homogeneously within the centre of the grains after 60-90mins and progresses towards the grain boundaries where there is a definitive precipitate free zone.

At both an ageing time of 90m and 4h, a Widmanstatten star morphology of the α phase within the β grains was observed (figure 4.13a and figure 4.14a). There was a uniform distribution of these small (up to 1µm), star-shaped particles which had precipitated homogeneously within the β matrix as well as along the grain boundaries. The volume fraction of these precipitates decreases with longer ageing times as they grow and evolve into other morphologies such as triangular or 'v' shapes. This is consistent with work conducted by Deghan-Manshadi and Dippenaar (2010) who studied the development of α phase morphologies during low temperature isothermal ageing of a Ti-5Al-5Mo-5V-3Cr alloy. The authors noted that each individual α precipitate is formed by a mesh of fine Widmanstatten plates. It was proposed that such plates are formed by a mechanism of sympathetic nucleation, that is, nucleation of a precipitate crystal at an interphase boundary of a crystal of the same phase. In particular, it is suggested that decomposition of the β phase begins by formation of the large plates of α, followed by an edge-to-face sympathetic nucleation of the smaller side plates onto the existing plates.
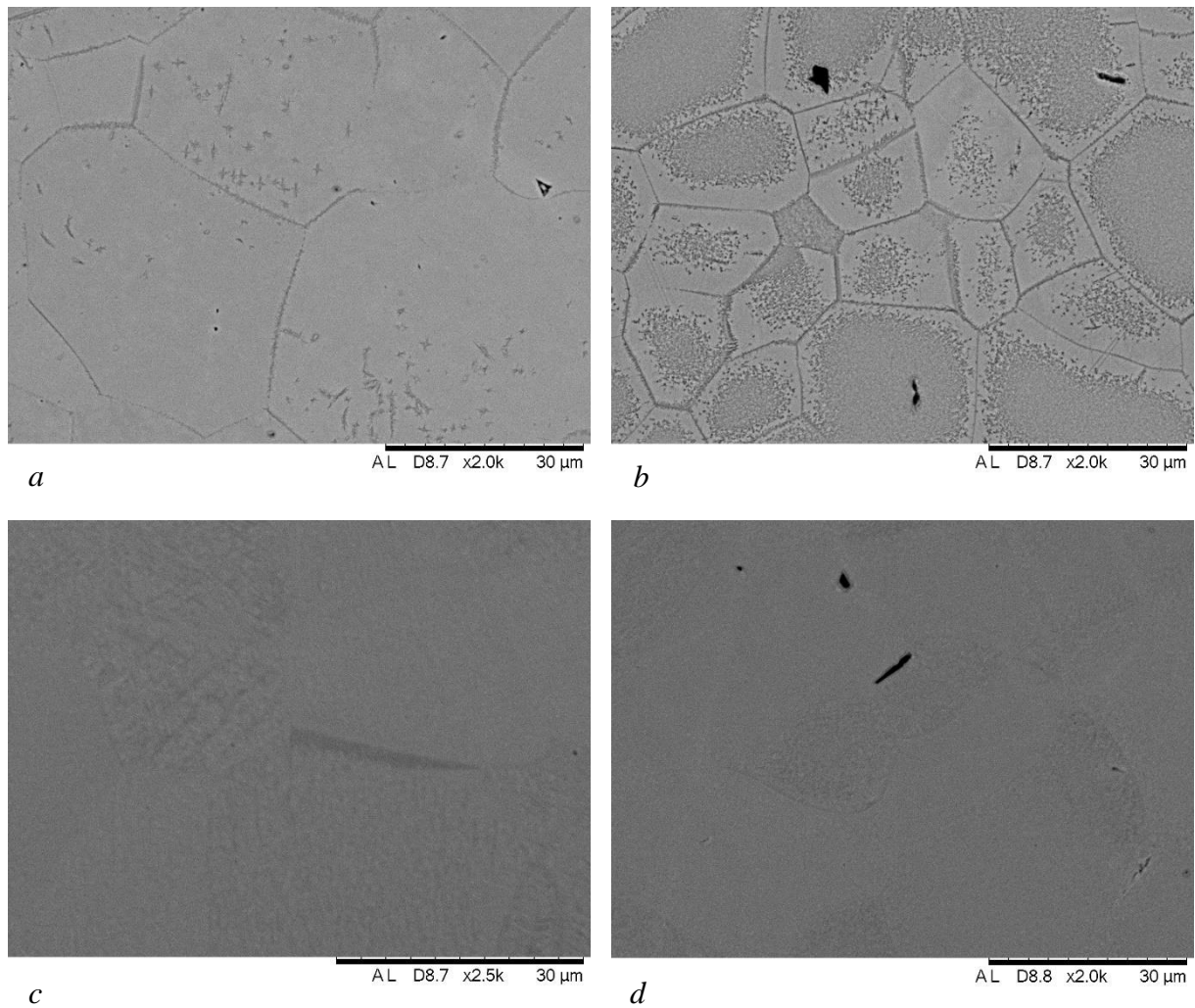
Figure 4.13: SEM images of 450°C aged samples at 2000x magnification: (a) 90m, (b) 4h, (c) 24h and (d) 9d

After an ageing time of 8 hours, the precipitates exhibit a lenticular morphology and are up to 1µm in length (figure 4.14c). There is a predominately continuous, thin layer of α along the grain boundaries with precipitates significantly coarser than those towards the centre of the grains. Interestingly, a number of precipitates in the vicinity of the grain boundaries exhibited a triangular or 'v' shaped morphology. This has been reported by several similar studies, such as that by Rhodes and Williams (1975), who noted the presence of a 'triangular phase' during low temperature ageing at 573K. A similar study by Miyano, Norimura, Inaba, and Ameyama (2006) demonstrated that each triangular α phase is composed of three individual α precipitates which exhibit a specific orientation with the β matrix and near-twin relationship with each other. The formation of these triangular or 'v' shaped morphologies is reportedly caused by sympathetic nucleation.
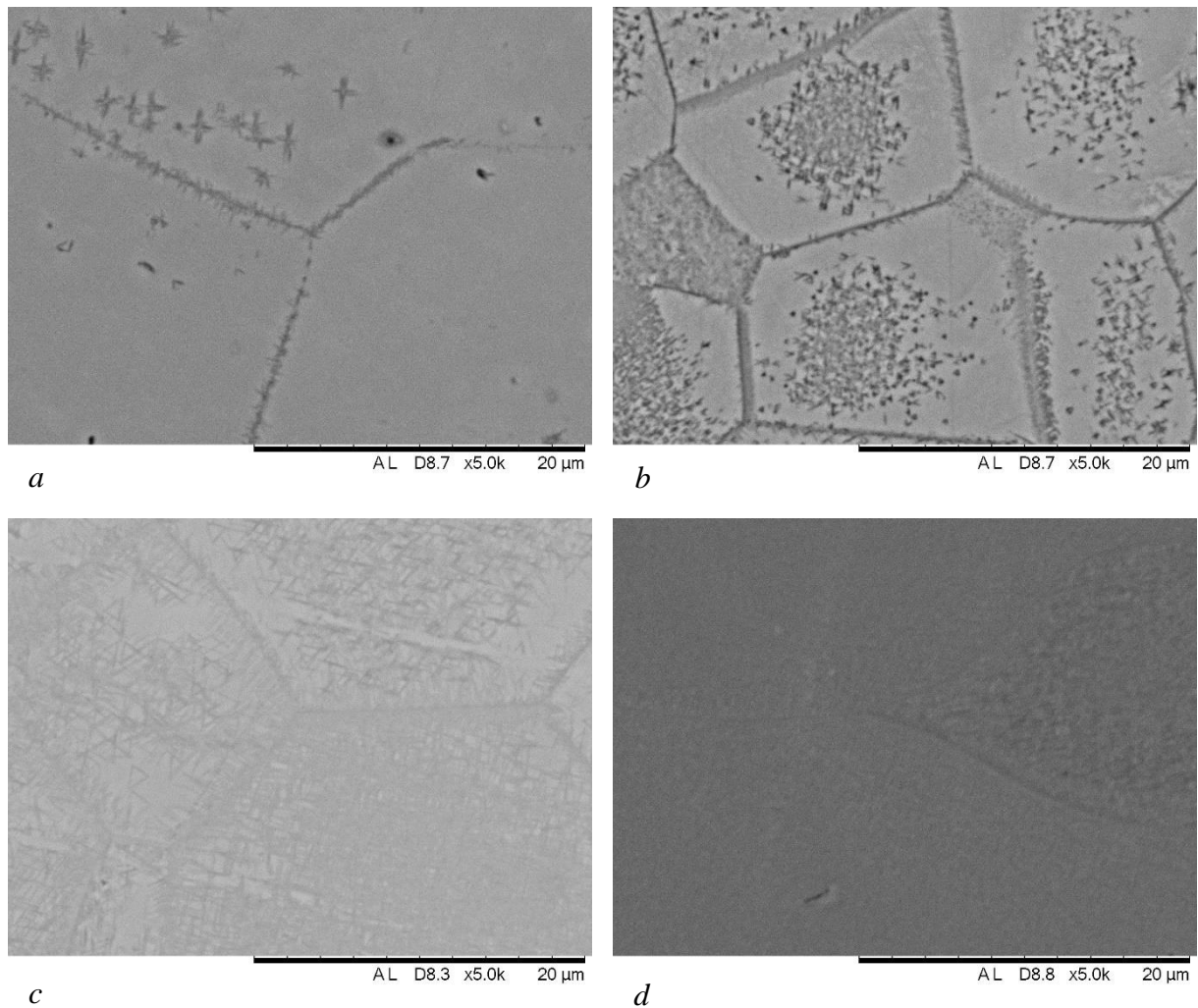
Figure 4.14: SEM images of 450°C aged samples at 5000x magnification: (a) 90m, (b) 4h, (c) 8h and (d) 9d

The lenticular morphology of the α precipitates is evident up to an ageing time of 9 days, with slight coarsening observed. The precipitate free zones adjacent to the grain boundaries reduce in size as an equilibrium volume fraction of α is obtained between 24 and 72 hours.

The results of the scanning electron microscopy for the 300°C isothermal ageing reveal very little about the size and morphology of the equilibrium α phase precipitates as they are much finer than the available resolution. In keeping consistent with the optical microscope results, the grains are fully β phase over an incubation period of 24-72 hours before equilibrium α precipitates are initiated. These are significantly smaller than 1µm in size and have a fine dispersion throughout the β matrix. Growth of larger precipitates is isolated to a few, select individual grains where rejection of α phase stabilising elements has occurred.
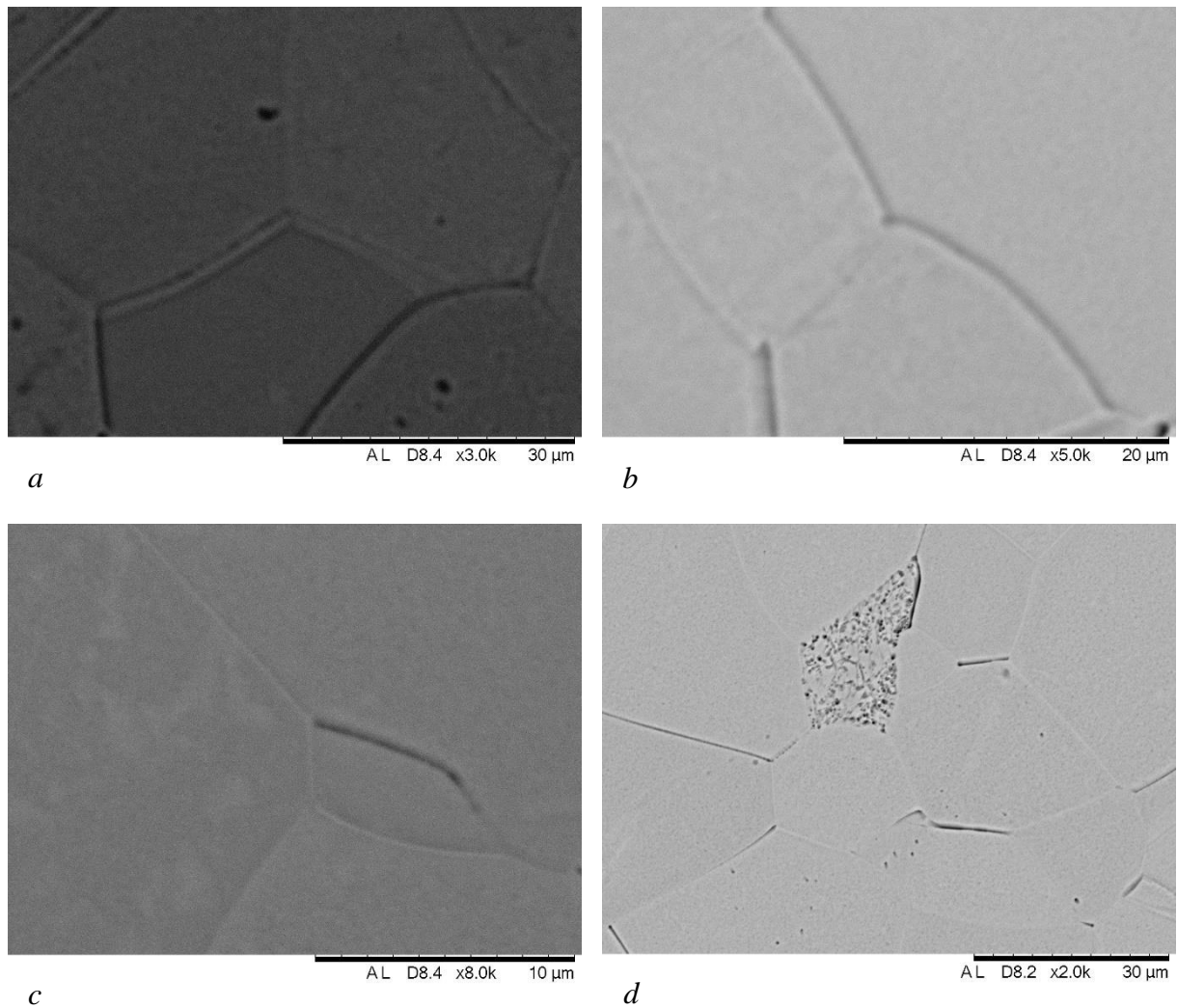
Figure 4.15: SEM images of 300°C aged samples: (a) 90m, (b) 24h, (c) 72h and (d) 9d

It is possible that the fine dispersion of α precipitates is due to the formation of metastable, transition phase particles which act as precursors for nucleation when there is insufficient thermal energy to decompose the β phase directly to equilibrium α. The phase which forms, either ω or β', is dependent on the alloying content and can only be determined by means of a higher level characterisation technique such as TEM or transmission electron microscopy. In the case where ageing is conducted above the temperature for the formation of ω or β' precipitates, there is an increased likelihood for nucleation of α particles as side plates at α/β interfaces. This is a point of comparison to the 450°C aged samples.

4.2 Microhardness Testing

The following figures 4.16 and 4.17 show the results of the microhardness testing for both ageing temperatures of 300 and 450°C with appropriate error bars delineating one standard deviation of the data. Hardening of the alloy under both conditions was observed over the 9day period due to the precipitation of fine α phase particles, however the ageing behaviour was notably different. In the case of the 450°C aged samples, a high rate of hardening was observed after an incubation period of 60mins with a maximum hardness value of 491Hv obtained at 72hours. This was a 71% increase when compared to the as received, solution treated sample. Over-ageing was noted in the 9day sample, which exhibited a hardness reading of 462Hv. In comparison, the 300°C aged trial has a much longer incubation period of up to 8hrs before any increase in the alloy's hardness and a plateau or peak hardness is not obtained after 9days of ageing. A maximum value of 405Hv, representing a 41% increase in hardness from the as received sample, is noted.
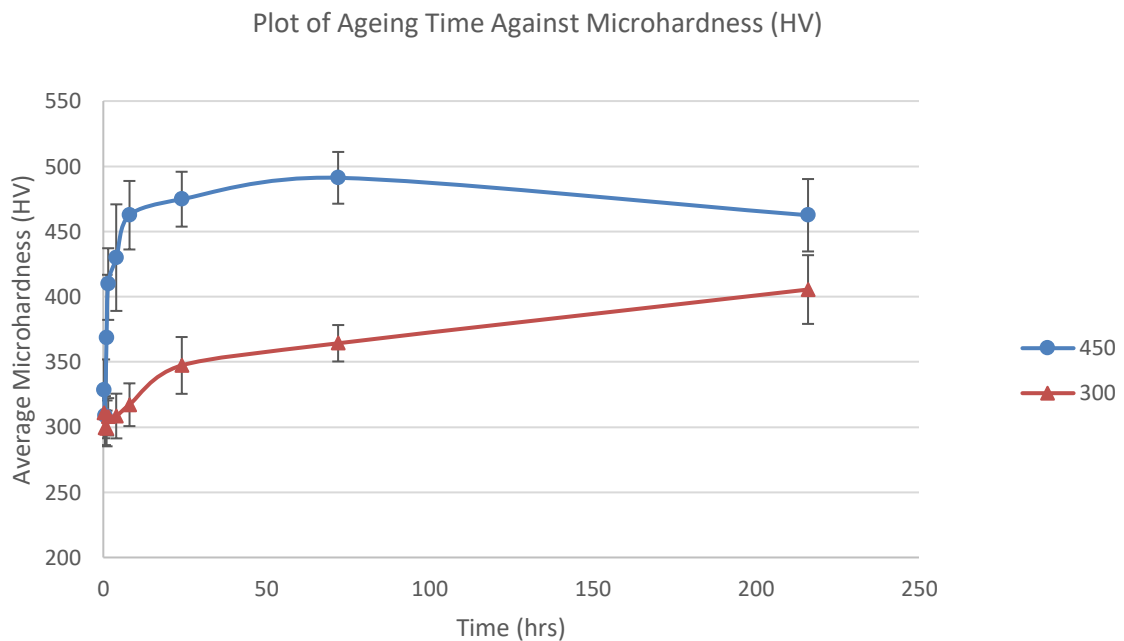

Figure 4.16: Age-Hardening Response of β-21S Titanium Alloy over 9day Period

Plot of Ageing Time Against Microhardness (HV)
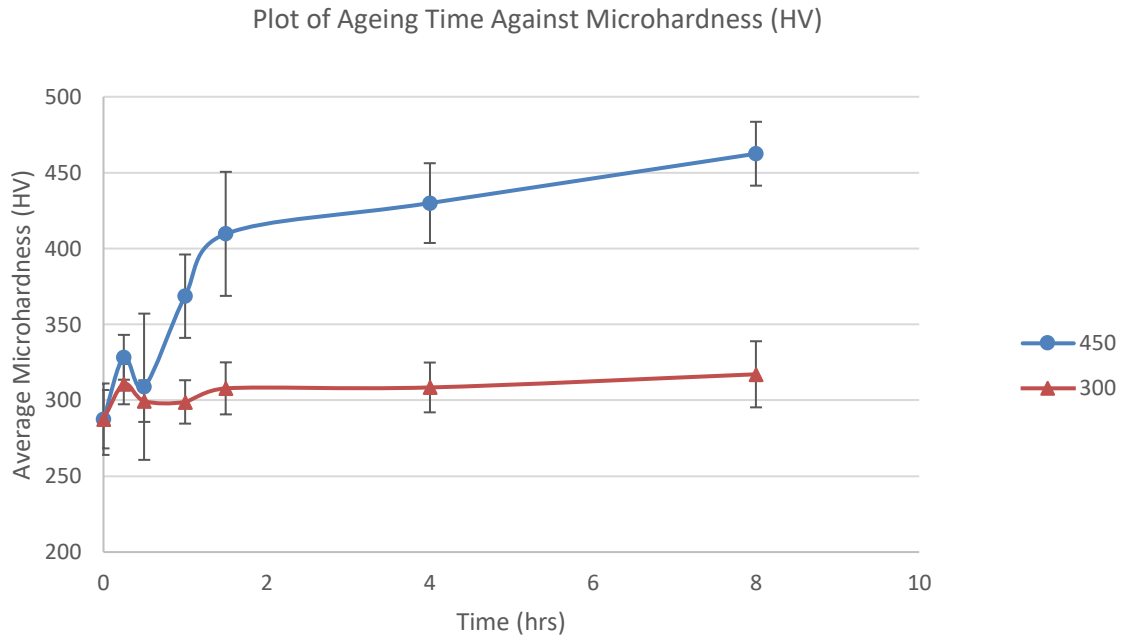
Figure 4.17: Age-Hardening Response of β-21S Titanium Alloy over Initial, 8hr Period

The hardness, and indeed the microhardness, is dependent on the precipitation of the equilibrium α phase precipitates and their ability to inhibit dislocation glide. This is in keeping with classical precipitation hardening theory; fine, hard particles within the microstructure result in greater resistance to dislocation slip and therefore have a higher hardening effect. More effective hardening is possible at lower ageing temperatures due to finer, more dense particles approaching the critical dispersions required for maximum strength. In the case of the 300°C samples, the microstructure is composed of a uniform, fine dispersion of α phase particles within the β matrix after 24hrs. This results in increasing hardness values up to a maximum of 405Hv at 9days with no plateau or over-ageing phenomenon observed. It was hypothesised from theory that an intermediate phase, ω or β', may have formed first due to insufficient thermal energy to directly decompose the β phase to equilibrium α. This lack of thermal energy – the rate of precipitation is dependent on the diffusion of solute elements – resulted in an incubation period of 8 hours. The hardness values increased by less than 10% during this period, which is within the bounds of identified uncertainty.

In comparison to the 300°C case, the 450°C aged samples experience a much more dramatic increase in hardness with an incubation period of 60mins. After 90mins, where large Widmanstatten star precipitates are observed, fine particles of the equilibrium α phase nucleate within the centre of the grains and grow rapidly in volume fraction as they progress towards the

grain boundaries. As a result, a hardness value of 462Hv is achieved after only 8hrs. After this point, the alloy's hardness begins to plateau as the α precipitates reach a critical dispersion and size. These precipitates have a lenticular structure and coarsen over time as larger particles grow preferentially to smaller ones. Over-ageing is observed after 9days, whereby the hardness value drops from a maximum 491Hv to 462Hv. This is again related to precipitation hardening theory with coarsening of the α phase ensuring that some particles can no longer be cut by dislocations, which instead bypass the precipitates.

4.3 Characterisation of Mechanical Properties

For titanium alloy β-21S, the mechanical properties are directly dependent on such factors as the morphology, volume fraction, size and distribution of the α phase in the β matrix, following formation during isothermal ageing below the β transus temperature. In particular, the fine, hard equilibrium α precipitates provide resistance to dislocation glide which increases the material yield strength and hardness. There is a linear relationship between these two properties, as described by equation 2.3 which approximates the yield stress as 1/3 of the material hardness (Hv), which has been validated by several similar studies such as that by Wang et al. (2012) who characterised the mechanical properties of β titanium alloy 6554.

In the 300°C samples, a peak hardness value of 405Hv ($\sigma_y \approx$ 1215MPa) is obtained after an ageing time of 9days. This is related to the microstructure which exhibits a uniform, fine dispersion of α precipitates within the β matrix. The growth of this phase is relatively slow due to insufficient thermal activation energy, meaning small atomic mobility and diffusion rate. There is an incubation period of up to 8hrs characterised by low hardness and strength. Given the minimal thermal energy for direct decomposition of the β phase to equilibrium α, it is likely that an intermediate phase, ω or β', may have formed first. This mechanism results in more dense particles approaching the critical dispersions required for maximum strength, as evidenced in the 72hr and 9day ageing trials. As plateauing of the hardness was not observed, it is likely that longer ageing times will result in further increases in strength. However, precipitate density may be limiting.

There is a much greater increase in the alloy strength during isothermal ageing at 450°C, with a peak hardness of 491Hv ($\sigma_y \approx$ 1473MPa) obtained after 72 hours. Rapid increases in strength are obtained after 90mins as fine α particles nucleate within the centre of the grains and progress

towards the grain boundaries. After ageing for 8hrs, characterised by lenticular α precipitates, the strength begins to plateau towards a peak value at 72hrs. Over-ageing is observed after this point as coarsening of the α phase occurs, ensuring that some particles can no longer be cut by dislocations, which instead bypass the precipitates.

The ductility of the alloy, or the degree of plastic deformation prior to fracture, is intrinsically linked to the hardness and yield strength due to the ability of the microstructure to resist dislocation slip. The fine α precipitates observed in the centre of the grains under both ageing conditions are expected to impede slip or plastic deformation and lead to a more brittle failure mode. Equally, a precipitate free zone adjacent to the grain boundaries was observed and is also expected to have a significant effect of the alloy ductility. Luterjing and Williams (2007) examined the mechanical properties of β titanium alloy 6246 and observed that localised increases in dislocation slip length in these 'soft' regions lead to a substantial pile-up of dislocations and subsequent crack nucleation.

Another important observation of the microstructure of the 450°C aged alloy was the presence of coarser and more widely dispersed precipitates in the vicinity of the grain boundaries. This is also hypothesised to lead to local increases in available slip length, therefore causing micro-crack formation. This phenomenon was noted by Shi et al. (2015) for a TC21 titanium alloy during tensile testing. The authors also observed that fine α precipitates can be cut by a dislocation along a crystal plane, allowing collective slip and therefore coplanar slip, which also causes micro-crack formation. This is a potential mechanism of fracture for the alloy under both ageing conditions.

4.3.1 Implications of Mechanical Properties for In-Service Behaviour

Although addressing the suitability of β-21S for any specific industry application(s) is outside of the scope of the project, it is important to speak to the research motivation of characterising the microstructure and mechanical properties for the purpose of describing in-service behaviour. Significant increases in the hardness and strength of the alloy at service temperatures of both 300 and 450°C are proportional to a decrease in the ductility with the potential for brittle failure. This is in part due to the formation of fine α precipitates within the grains which impede dislocation slip and therefore plastic deformation. A critical hardness and/or strength was observed at 72hours in the case of the 450°C trial whilst no over-ageing was noted at 350°C. It

is plausible that the strength of the alloy could increase with further ageing. The presence of precipitate free zones at the grain boundaries may result in localised increases in dislocation slip length in these 'soft' regions, resulting in dislocation-pile up and crack nucleation. This mechanism is also expected to have an effect on the 450°C aged samples due to the presence of coarser and more widely dispersed precipitates in this vicinity which can enlarge slip length.

Chapter 5

Conclusions and Recommendations

5.1 Statement on Achievement of Aim

This section begins with a restatement of the overall aim or objective of the thesis; "The aim of this body of work is to investigate the changes in microstructure and mechanical properties during thermal ageing of solution treated β-21S titanium alloy." Using optical microscopy and SEM techniques, the changes in microstructure were characterised across discrete time periods of up to 9days and for isothermal ageing temperatures of 300 and 450°C. The effects of such microstructural changes were quantified through the use of microhardness testing, with experimental data expected to exhibit a close relationship to the alloy's yield strength and ductility. This enabled potential modes of in-service failure, including the likelihood of embrittlement and cracking, to be hypothesised.

5.2 Summary of Research Outcomes

Isothermal ageing at 300°C of titanium β-21S resulted in a fine, uniform dispersion of α precipitates within the β matrix after an ageing time of 9days. This corresponded to a peak hardness value of 405Hv ($\sigma_y \approx 1215$MPa). This is in keeping with precipitation hardening theory; fine, hard particles of equilibrium α within the matrix provide resistance to dislocation glide and plastic deformation. The growth of the equilibrium α phase is relatively slow due to insufficient thermal activation energy, meaning small atomic mobility and diffusion rate. An incubation period of up to 8hrs is characterised by low hardness. It is hypothesised, due to insufficient thermal energy for direct decomposition of the β phase to equilibrium α, that an intermediate phase, ω or β', may have first formed. These nano-sized transitional phase precipitates serve as precursors for the nucleation of α platelets, therefore resulting in a denser aggregate of particles which approach the critical dispersions required for maximum strength.

In comparison, the 450°C aged samples exhibited a rapid increase in hardness after only 60mins, with a peak value of 491Hv ($\sigma_y \approx 1473$MPa) obtained at 72hours. After 4hrs, a Widmanstatten star-shaped morphology or clustering of fine α plates was observed throughout

the matrix as well as at the grain boundaries. Fine dispersions of α nucleated within the centre of the grains with growth towards the grain boundaries as the volume fraction increases. It is unsure whether the formation of this phase is due to direct precipitation of equilibrium α, nucleation as an extension of a transitional phase, decomposition of the Widmanstatten star morphology or a combination of each. The precipitates exhibit a lenticular structure after 8hrs and are observed to coarsen over time as larger particles grow preferentially to smaller ones. This results in over-ageing after 9days as some particles can no longer be cut by dislocations, which instead bypass the precipitates.

The fine dispersions of equilibrium α observed under both ageing conditions, particularly after 4hrs at 450°C and 24hrs at 300°C, are expected to impede dislocation slip or plastic deformation such that high strength at the expense of ductility will result. This is evidenced by the microhardness results. At both temperatures, a precipitate free zone adjacent to the grain boundary was observed and has been shown in previous studies to result in micro-cracking under load as increases in dislocation slip length in these 'soft' regions lead to a substantial pile-up of dislocations. This is also a plausible mode of failure during ageing at 450°C as coarser and more widely dispersed precipitates in the vicinity of the grain boundaries increase dislocation slip length.

5.3 Discussion of Experimental Uncertainty

A number of factors were seen to limit the efficacy of the investigation and/or contribute to the propagation of experimental uncertainty. These include:

- Work hardening at the sample surface due to the shear stress imposed by the guillotine. This may have resulted in twinning and was not completely removed during grinding and polishing.
- Slight changes in the bounds of measurement during microhardness testing which are known to produce widely different results. A maximum standard deviation of 48Hv (11% uncertainty) was noted, suggesting fairly good consistency.
- Retention of micro-sized droplets of OP-S suspension, particularly at lower ageing times, reducing the clarity of microscopy images. The same was true for staining at the metal/mould interface.
- Level of characterisation of optical microscope and SEM techniques.

- Approximations of such mechanical properties as yield strength, ultimate tensile strength and ductility from microhardness results and microstructural features.

5.4 Recommendations for Continuation, Improvement and Publication

It is anticipated that the current body of work will result in publication in the near future. In particular, Dr. Michael Bermingham has been working with two additional students to gather microscopy and microhardness data for ageing temperatures of 350, 400, 500 and 550°C. Collectively, this data will be used to construct a journal publication describing the low temperature ageing response of the metastable β titanium alloy Ti-15 Mo-3 Nb-3 Al- 0.2 Si. A sketch-up of such a publication is provided in appendix B. This body of work lends itself to being published as there exists little to no knowledge in the public domain regarding the metallurgical stability or ageing response of the β-21S alloy over such a temperature range.

Despite expected publication, a number of recommendations for continuation and improvement of the current body of work have been identified. Firstly, it is suggested that a higher level characterisation technique such as transmission electron microscopy (TEM) or x-ray powder diffraction (XRD) be used to investigate the formation of the intermediate phase precipitates ω and/or β'. It would also be of benefit to better understand the nucleation process of the Widmanstatten star and triangular precipitates observed during ageing at 450°C. Another beneficial addition to the research would be the use of tensile testing to directly measure such properties as the yield strength, ultimate tensile strength and degree of plastic deformation prior to failure. These properties were inferred from microhardness results, which is common practice and justifiable, but not ideal.

In conjunction with the tensile testing, future work could investigate the likelihood and/or mechanism of crack nucleation in the precipitate free zones adjacent to the grain boundaries, which has previously been shown to result due to increases in dislocation slip length leading to pile-up. Other mechanisms causing micro-crack formation, including coplanar slip due to the cutting of fine α precipitates and increases in dislocation slip length where coarse and widely dispersed particles persist, should similarly be investigated.

Bibliography

Agarwal, N., Bhattacharjee, A., Ghosal, P., Nandy, T.K., & Sagar, P.K. (2008). Heat Treatment, Microstructure and Mechanical Properties of a Metastable β Titanium Alloy Timetal 21S. *Transactions of the Indian Institute of Metals, 61*, 419-425. doi: 10.1007/s12666-008-0074-6

Chaudhuri, K., & Perepezko, J.H. (1994). Microstructural Study of the Titanium Alloy Ti-15Mo-2.7Nb-3Al-0.2Si (Timetal 21S). *Metallurgical and Materials Transactions A, 25A*, 1109-1118. doi: 10.1557/JMR.1997.0110

Coakley, J et al. (2015). Precipitation Processes in the Beta Titanium Alloy Ti-5Al-5Mo-5V-3Cr. *Journal of Alloys and Compounds, 646*, 946-953. doi: 10.1016/j.jallcom.2015.05.251

Deghan-Manshadi. A., Dippenaar, R. (2010). Development of Alpha-Phase Morphologies During Low Temperature Isothermal Heat Treatment of a Ti–5Al–5Mo–5V–3Cr Alloy. *Materials Science and Engineering, 528*, 1833-1839. doi: 10.1016/j.msea.2010.09.061

Gouda, M.K., Nakamura, K., & Gepreel, M.A.H. (2015). First Principles Study on the Effect of Alloying Elements on the Elastic Deformation Response in β-Titanium Alloys. *Journal of Applied Physics, 117*, 214905. doi: 10.1063/1.4921972

Huang, X., Cuddy, J., Goel, N., & Richards, N.L. (1994). Effect of Heat Treatment on the Microstructure of a Metastable β-Titanium Alloy. *Journal of Material Engineering and Performance, 3*, 560-566. doi: 10.1007/s11041-014-9740-y

Ivasishin, O.M., & Teliovich, R.V. (1999). Potential of Rapid Heat Treatment of Titanium Alloys and Steels. *Materials Science and Engineering: A, 263*, 142-154. doi: 10.1016/S0921-5093(98)01173-3

Kent, D., Wang, G., Wang, W., & Dargusch, M.S. (2012). Influence of Ageing Temperature and Heating Rate on The Properties and Microstructure of β Titanium Alloy, Ti-6Cr-5Mo-5V-4Al. *Materials Science and Engineering: A, 531*, 98-106. doi: 10.1016/j.msea.2011.10.040

Kent, D., Wang, G., & Dargusch, M. (2013). Effects of Phase Stability and Processing on the Mechanical Properties of Ti-Nb Based β Titanium Alloys. *Journal of Mechanical Behaviour of Biomedical Materials, 28*, 15-25. doi: 10.1016/j.jmbbm.2013.07.007

Leyens, C., & Peters, M. (2003). *Titanium and Titanium Alloys, Fundamentals and Applications*. Weinheim: Wiley-VCH

Luterjing, G., & Williams, J.C. (2007). *Titanium*. Hamburg: Springer Berlin Heidelberg

Mantri. S et al. (2015). Influence of Fine-Scale Alpha Precipitation on the Mechanical Properties of the Beta Titanium Alloy Beta-21S. *Metallurgical and Materials Transactions A, 46,* 2803-2808. doi: 10.1007/s11661-015-2944-y

Miyano, N., Norimura, T., Inaba, T., & Ameyama, K. (2006). Reasons for the Formation of Triangular α Precipitates in Ti-5V-3Cr-3Sn-3Al β Titanium Alloy. *Materials Transactions, 47*, 341-347. Retrieved from http://www.jim.or.jp/journal/j/

Morris, J.W. (2001). *Dislocation Plasticity: An Overview*. Amsterdam: Elsevier Science

Polmear, I. (2005). *Light Alloys from Traditional Alloys to Nanocrystals*. Burlington: Elsevier Science

Rhodes, C., & Williams, J. (1975). Precipitation of Alpha-phase in Metastable Beta-phase Ti Alloys. *Metal Transactions 6A, 11*, 2103-2114. Retrieved from https://inis.iaea.org/

Shi, Z., Guo, H., Liu, R., Wang, X., & Yao, Z. (2015). Microstructure and Mechanical Properties of TC21 Titanium Alloy by Near-Isothermal Forging. *Transactions of Non-Ferrous Metals Society of China, 25*, 72-79. doi: 10.1016/S1003-6326(15)63580-4

Smart, M. MECH2300 Lecture on Precipitation Hardening. Presented at The University of Queensland, Brisbane, August 12, 2013

Wanhill, R., & Barter, S. (2012). *Fatigue of Beta Processed and Beta Heat Treated Titanium Alloys*. London: Springer

Zhang, M. MECH3305 Lecture on Phase Transformations. Presented at The University of Queensland, Brisbane, October 10, 2015

Zhao, Y.Q., Xin, S.W., & Zeng, W.D. (2009). Effect of Major Alloying Elements on Microstructure and Mechanical Properties of a Highly β Stabilised Titanium Alloy. *Journal of Alloys and Compounds, 481*, 190-194. doi: 10.1016/j.jallcom.2009.03.042

Appendix

A - Raw Microhardness Data

Table A.1: Raw Microhardness Data

| Heat Treatment | Hardness Vickers (Hv) | | | | | | | | | | | | | | |
	1	2	3	4	5	6	7	8	9	10	11	12	13	14	15
As Supplied	282	299	292			269	284	289			276	305	292		
300 - 15m	294	297	291	283	304	359	303	342	320	314	315	307	313	307	311
300 - 30m	333	285	298	300	298	297	302	316	307	297	274	304	292	297	292
300 - 60m	339	304	290	304	313	286	287	296	304	291	292	286	303	297	292
300 - 90m	313	313	321	315	323	303	303	307	311	309	299	301	268	301	331
300 - 4h	344	307	307	322	307	293	307	284	300	307	292	344	294	308	311
300 - 8h	294	339	309	310	311	332	311	351	332	321	317	321	288	312	309
300 - 24h	327	313	392	333	333	322	344	359	344	339	379	361	343	349	371
300 - 72h	356	370	376	362	361	350	362	346	390	359	369	360	395	349	359
300 - 9d	439	396	361	376	383	443	420	452	423	419	389	385	393	403	400
450 - 15m	373	350	350	330	342	307	286	324	307	301	312	338	355	319	331
450 - 30m	343	324	300	311	317	300	317	318	312	304	313	295	291	282	307
450 - 60m	353	455	315	468	310	386	411	325	350	386	367	308	375	367	353
450 - 90m	410	432	432	408	418	431	446	349	410	410	400	437	354	400	408
450 - 4h	402	482	402	507	460	375	375	368	429	409	444	460	455	439	442
450 - 8h	531	463	445	480	491	451	442	468	431	433	466	478	466	458	434
450 - 24h	529	482	479	478	472	471	493	467	482	473	491	447	444	462	451
450 - 72h	496	509	515	500	506	498	475	479	488	479	442	499	515	467	499
450 - 9d	485	443	436	439	438	445	474	462	427	449	428	490	484	504	484

B - Outline of Journal Publication

It is anticipated that the current body of work will result in publication in the near future. Dr. Michael Bermingham has been working with two additional students to gather microscopy and microhardness data for ageing temperatures of 350, 400, 500 and 550°C. Collectively, this data will be used to construct a journal publication describing the low temperature ageing response of the metastable β titanium alloy Ti-15 Mo-3 Nb-3 Al- 0.2 Si. This body of work lends itself to being published as there exists little to no knowledge in the public domain regarding the metallurgical stability or ageing response of the β-21S alloy over such a temperature range. Collaboration with Dr. Damon Kent is expected in order to finalise the publication, which is presented in a draft form below.

Characterising the Microstructure and Mechanical Properties of a Ti-15Mo-3Nb-3Al-0.2Si Alloy During Low Temperature Ageing

M. Bermingham[a], D. Kent[b], P. Hagan[a], P. Chesters[a], M. Campbell[a]

School of Mechanical and Mining Engineering, The University of Queensland, Brisbane, QLD 4072, Australia

ARTICLE INFO

ABSTRACT

The changes in the microstructure and mechanical properties of an aerospace β-21S titanium alloy (Ti-15 Mo-3 Nb-3 Al- 0.2 Si) have been studied during low temperature thermal ageing (300-550°C). The development of the morphologies of α phase precipitates was observed to vary significantly across isothermal ageing temperatures and times. Ageing of the alloy between 400 and 450°C resulted in fine dispersions of α nucleated within the centre of the grains which rapidly grow towards the grain boundaries over time. This corresponded to the greatest age hardening response after 72hrs (491Hv). At 300°C, growth of the equilibrium α phase is relatively slow due to insufficient thermal activation energy, meaning small atomic mobility and diffusion rate. It is hypothesised that an intermediate phase, ω or β', may have first formed. The degree of strengthening declined at greater ageing temperatures due to coarsening of the precipitate morphologies (maximum 385Hv).

1. Introduction
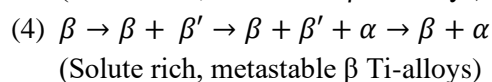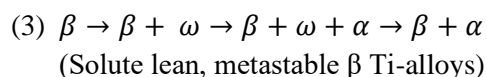
Titanium β-21S or Timetal 21S is a metastable β alloy with designation Ti-15 Mo-3 Nb-3 Al-0.2 Si and is designed for high temperature applications, such as in aircraft engine exhaust plug and nozzle assemblies, due to its improved oxidation and creep resistance. The addition of alloying elements Nb, Al and Si to the Ti-Mo system are specifically targeted at improving oxidation resistance [1]. Currently, there exists little to no knowledge in the public domain regarding the metallurgical stability or ageing

response of this alloy over typical operating temperatures of 200-600°C.

In metastable β titanium alloys, several phase transformations can take place with each influenced by the alloy composition and ageing temperature. An equilibrium alpha phase forms during isothermal ageing below the β transus temperature as well as during slow cooling from the β field [2]. The direct decomposition of the β phase to equilibrium α is observed only at sufficiently large temperatures due to the difficulty of nucleating HCP α phase from the BCC β matrix. Consequently, intermediate decomposition products or transitional phases are often formed.

An ω phase may form during quenching (athermal ω) or during low temperature ageing (isothermal ω) [3]. The morphology of this phase is heavily dependent on the misfit between the precipitate and BCC structure of the matrix. In low misfit alloys, an ellipsoidal ω phase persists whilst in high misfit alloys a cuboidal phase is formed. It was also found that in alloys with β stabilising elements, a β' transitional phase is formed. This is due to the separation of the BCC phase into two BCC phases of different compositions in these alloys [4]. If silicon is an alloying element, silicides may also be found. Low temperature ageing can therefore be said to result in the following two phase transformations, depending on ageing time and temperatures [3, 5]:

(3) $\beta \rightarrow \beta + \omega \rightarrow \beta + \omega + \alpha \rightarrow \beta + \alpha$
   (Solute lean, metastable β Ti-alloys)

(4) $\beta \rightarrow \beta + \beta' \rightarrow \beta + \beta' + \alpha \rightarrow \beta + \alpha$
   (Solute rich, metastable β Ti-alloys)

Microhardness testing was seen as a viable technique by which to efficiently ascertain the ageing behaviour of the alloy across several temperature and time combinations. As the alloy hardness is fundamentally related to the precipitation hardening response, it can therefore be used to estimate the strength.

2. Experimental Methods

A Ti-15 Mo-3 Nb-3 Al- 0.2 Si (% by mass) β-titanium alloy was received as a wrought sheet from which small samples (approximately 5x10x1mm) were cut. Isothermal ageing of the samples at both a specified furnace temperature of 300°C and 450°C was conducted for varying time periods (0, 0.25, 0.5, 1, 1.5, 4, 8, 24, 72 and 216 hours). Three samples were obtained for each temperature and time permutation. This was followed by air cooling to room temperature. Each group of samples was mounted in Bakelite resin. The Vickers microhardness of the samples was tested after a standard metallographic process of mechanical grinding and polishing. Five data points on each sample, amounting to fifteen for the specified temperature and ageing time, were obtained. The microstructural development of the alloy was examined by means of optical microscopy and scanning electron microscopy (SEM) following etching in Kroll's reagent.

3. Discussion of Experimental Results

Preliminary microhardness results collated from all of Dr. Michael Bermingham's students show the ageing response of titanium alloy β-21S at discrete temperature intervals of 50°C from 300 to 550°C (figure 3.1). At the lower ageing temperatures of 300 and 350°C, there is a significant incubation period before rapid increases in the hardness. This is related to the nucleation and growth of the equilibrium α phase, which is relatively slow due to insufficient thermal activation energy meaning small atomic mobility and diffusion rate. It is hypothesised that an intermediate phase, ω or β', may have first formed. These nano-sized transitional phase precipitates serve as precursors for the nucleation of α platelets where there is insufficient thermal energy for direct decomposition of the β phase to equilibrium α.
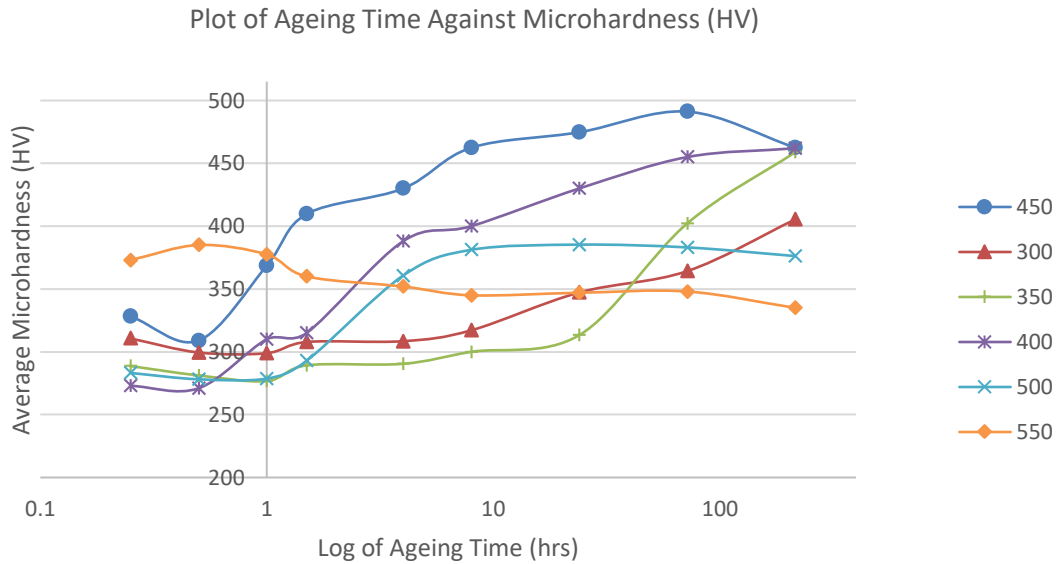
Plot of Ageing Time Against Microhardness (HV)

Figure B.1: Age-Hardening Response of β-21S Titanium Alloy over 9day Period

As the isothermal ageing temperature increases to 400 and 450°C, there is a much more severe increase in hardness which occurs at shorter ageing times. A peak in the hardness of approximately 450-500Hv occurs around 72hrs to 9days and is characterised by plateauing and then over-ageing as larger particles grow preferentially to smaller ones and can no longer be cut by dislocations. At ageing temperatures of 500 and 550°C, the peak hardness drops away significantly. One explanation is that the β phase had decomposed directly to equilibrium α, potentially forming coarse Widmanstatten plates which have only a moderate resistance to dislocation glide. The temperature is above that at which precipitation of the intermediate phase particles can occur. These nano-sized particles result in a denser aggregate of α precipitates which approach the critical dispersions required for maximum strength. Direct decomposition of β to equilibrium α is therefore likely to result in the nucleation of α particles as side plates at α/β interfaces. Although there is a greater diffusion rate at these temperatures, this at the expense of the potential volume free energy change.

The thickness of grain boundary α increased with ageing time and has been shown in previous studies to result in micro-cracking under load as increases in dislocation slip length in these 'soft' regions lead to a substantial pile-up of dislocations.

4. Summary

This study investigated the changes in the microstructure and mechanical properties of an aerospace β-21S titanium alloy (Ti-15 Mo-3 Nb-3 Al- 0.2 Si) during low temperature thermal ageing (300-550°C). The development of the morphologies of α phase precipitates was observed to vary significantly across isothermal ageing temperatures and times. Isothermal ageing between 300°C and 350°C of titanium β-21S resulted in a fine, uniform dispersion of α precipitates within the β matrix after an ageing time of 9days. This corresponded to a peak hardness value of 405Hv ($\sigma y \approx 1215$MPa). This is in keeping with precipitation hardening theory; fine, hard particles of equilibrium α within the matrix provide resistance to dislocation glide and plastic deformation. The growth of the equilibrium α phase is relatively slow due to insufficient thermal activation energy, meaning small atomic mobility and diffusion rate. An incubation period of up to 8hrs is characterised by low hardness. It is hypothesised, due to insufficient thermal energy

for direct decomposition of the β phase to equilibrium α, that an intermediate phase, ω or β', may have first formed.

In comparison, the 440 and 450°C aged samples exhibited a rapid increase in hardness after only 60mins, with a peak value of 491Hv (σy ≈1473MPa) obtained at 72hours. Fine dispersions of α nucleated within the centre of the grains with growth towards the grain boundaries as the volume fraction increases. The precipitates exhibit a lenticular structure after 8hrs and are observed to coarsen over time as larger particles grow preferentially to smaller ones. This results in over-ageing after 9days as some particles can no longer be cut by dislocations, which instead bypass the precipitates. The degree of strengthening declined at greater ageing temperatures of 500 and 550°C due to coarsening of the precipitate morphologies (maximum 385Hv).

Acknowledgements

References

[1]   Agarwal, N., Bhattacharjee, A., Ghosal, P., Nandy, T.K., & Sagar, P.K. (2008). Heat Treatment, Microstructure and Mechanical Properties of a Metastable β Titanium Alloy Timetal 21S. *Transactions of the Indian Institute of Metals*, 61, 419-425. doi: 10.1007/s12666-008-0074-6

[2]   Chaudhuri, K., & Perepezko, J.H. (1994). Microstructural Study of the Titanium Alloy Ti-15Mo-2.7Nb-3Al-0.2Si (Timetal 21S). *Metallurgical and Materials Transactions A*, 25A, 1109-1118. doi: 10.1557/JMR.1997.0110

[3]   Deghan-Manshadi. A., Dippenaar, R. (2010). Development of Alpha-Phase Morphologies During Low Temperature Isothermal Heat Treatment of a Ti–5Al–5Mo–5V–3Cr Alloy. *Materials Science and Engineering*, 528, 1833-1839. doi: 10.1016/j.msea.2010.09.061

[4]   Luterjing, G., & Williams, J.C. (2007). *Titanium*. Hamburg: Springer Berlin Heidelberg

[5]   Polmear, I. (2005). *Light Alloys from Traditional Alloys to Nanocrystals*. Burlington: Elsevier Science